



Rare-earth metal based adsorbents for effective removal of arsenic from water: A critical review

Yang Yu^{a,b}, Ling Yu^{b,c}, Kok Yuen Koh^b, Chenghong Wang^b, and J. Paul Chen^{b,d,e} 

^aGuangdong Key Laboratory of Environmental Pollution and Health, and School of Environment, Jinan University, Guangzhou, China; ^bDepartment of Civil and Environmental Engineering, National University of Singapore, Singapore; ^cSchool of Environmental Science and Engineering, Sun Yat-Sen University, Guangzhou, China; ^dTechnion-Israel Institute of Technology, Department of Chemical Engineering, Haifa 3200, Israel; ^eCollege of Engineering, Guangdong Technion Israel Institute of Technology (GTIIT), 243 Da Xue Road, Shantou, Guangdong, PR China

ABSTRACT

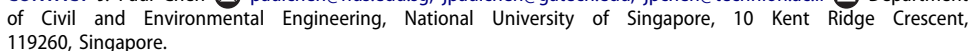
Arsenic contamination is a global environmental problem due to arsenic's high toxicity, bioaccumulation in human body and food chain, and severe carcinogenicity to humans. Development of cost-effective remediation technologies is of importance due to the implementation of stricter regulation for drinking water. This review article focuses on the chemical properties and applications of three rare-earth metals (REMs, lanthanum, cerium, and yttrium) based adsorbents for arsenic removal. Among them, cerium (IV) based adsorbents are more efficient for simultaneous adsorption and oxidization of As(III) from the aqueous solutions, while the yttrium based adsorbents adsorb more arsenic than other REM based adsorbents. A series of studies has demonstrated that higher removal efficiency of arsenic can be obtained by the adsorbents that are fabricated by combination of the REMs with less costly and commonly existing metals such as iron and manganese. Faster adsorption can be achieved by using the REM doped support materials that have larger specific surface areas and greater porosity. Ligand exchange, and surface complexation play key roles in the adsorption. It is concluded that the REM based adsorbents can greatly outperform the conventional metal based adsorbents for the industrial applications of treatment of arsenic containing wastewater.

ABBREVIATIONS

3-D: Three dimensional; CHT: Chitosan; CNB: cellulose ultrafine nanobioadsorbent; CNT: Carbon nanotube; EDX: energy dispersive X-ray spectroscopy; EXAFS: extended X-ray absorption fine structure spectroscopy; E⁰: standard electrode potential; FESEM: field emission scanning electron microscopy; FTIR: Fourier transform infrared spectroscopy; GNP: graphene nanoplatelet; GO: graphene oxide; HCO: hydrous cerium oxide; HREEs: heavy rare-earth elements; LREEs: light rare-earth

KEY WORDS

Adsorption; applications; arsenic; ligand exchange; rare-earth metal; surface complexation

CONTACT J. Paul Chen  paulchen@nus.edu.sg, jpaulchen@gatech.edu, jpchen@technion.ac.il 

Color versions of one or more of the figures in the article can be found online at www.tandfonline.com/best.

elements; M: metal; Max.: maximum; MCL: maximum contaminant level; PAC: powdered activated carbon; Pu: Pumice; PVA: polyvinyl alcohol; Ref.: Reference; REM: rare-earth metal; Rs: Red scoria; TEM: transmission electron microscopy; USEPA: United States Environmental Protection Agency; XPS: X-ray photoelectron spectroscopy.

1. Introduction

Arsenic contamination in water has become a serious environmental problem in many regions of the world, including Argentina, Bangladesh, Canada, China, Chile, Hungary, India, Mexico, Nepal, Thailand, UK, United States, and Vietnam (Yu, Yu, & Chen, 2015). It is estimated that about 150 million people are exposed to arsenic contaminated drinking water (Ravenscroft, Brammer, & Richards, 2009).

Arsenic can exist in different types of water bodies as a result of both natural processes and anthropogenic activities. Such natural conditions as weathering, leaching of arsenic from arsenic-rich minerals, biological processes, and atmospheric deposition cause the release of arsenic into the water. With rapid industrialization in many countries in the last 150 years, in particular, China in the last 30 years, higher risks from arsenic contamination have been posed by anthropogenic activities such as agriculture, mining, and industrial discharge of arsenic-containing wastewaters (Shukla, Dubey, Singh, Tajbakhsh, & Chaudhry, 2010; Wang & Mulligan, 2006).

Arsenate (As(V)) and arsenite (As(III)) are the most common inorganic arsenic species in the environment. As(V) usually exists in well-oxygenated water, while the highly toxic As(III) is mainly in anaerobic water (Rahman, Rahman, Samad, & Alam, 2008). Since As(III) is more difficult to be removed than As(V), As(III) is normally oxidized to As(V) first and subsequently removed.

Due to the higher toxicity and bioaccumulation, arsenic in drinking water can cause a series of severe health problems, such as hyperkeratosis, hyperpigmentation, disturbance in the peripheral vascular and nervous system; more importantly, excess intake of arsenic can even cause several cancers in the main human organs such as the skin, lungs, kidney, bladder, liver, and prostate (Mazumder et al., 1998; Anawar, Akai, Mostofa, Safiullah, & Tareq, 2002; Hall, 2002; Kapaj, Peterson, Liber, & Bhattacharya, 2006). Therefore United States Environmental Protection Agency (USEPA) decided to reduce the maximum contaminant level (MCL) of arsenic from 50 to 10 $\mu\text{g/L}$ in drinking water, in early 2006.

The most common and available technologies for arsenic removal include coprecipitation (Wang, Gong, Liu, Liu, & Qu, 2011), ion exchange

(He, Tian, & Ning, 2012; Kim & Benjamin, 2004), membrane filtration (Sabbatini et al., 2010, Wang et al., 2016; Yu, Zhao, Wang, Fan, & Luan, 2013), and adsorption (Wang, Liu, Chen, & Li, 2015; Wei, Zheng, & Paul Chen, 2011; Zheng, Yu, Wu, & Paul Chen, 2012). Occasionally, biological technologies were reportedly used in the treatment of arsenic containing wastewater (Srivastava et al., 2011).

Recently, more attention has been given on the applications of the adsorbents prepared by several rare-earth metals (REMs) for the water treatment due to their favorable chemical properties. Compared to typically used metals (e.g., iron, aluminum, and manganese), the adsorbents prepared by the REMs have more functional groups on their surfaces (Yu, Yu, Sun, & Chen, 2016), and better catalysis reaction performance (Miao et al., 1997), which are favorable for arsenic uptake. In addition, they have no or lower toxicity for humans. A series of REM based adsorptive materials in forms of metal oxides/hydroxides, metal oxide/hydroxide modified adsorbents and metal ion impregnated adsorbents have been recently reported for the effective decontamination of arsenic.

This review article is to provide an overview on recent studies on the development and applications of REM typed adsorbents for arsenic removal in laboratory or large scales. A brief introduction on REMs and their properties is first given. A comparison of REM based adsorbents and commonly used metal based adsorbents (e.g., iron based) is provided to demonstrate the advantages of the first type adsorbents over the second type adsorbents on the adsorptive removal of arsenic. The shortcomings of the adsorbents are discussed.

2. Rare-earth metals and their characteristics

The REMs are defined as the group of the 17 metallic elements with similar chemical properties including lanthanides, scandium, and yttrium. Since Carl Axel Arrhenius discovered a black mineral “Ytterbite” in 1787, the REMs have gradually become known to the world in the following years.

The lanthanides, as a series of elements with atomic numbers of 57 to 71, are generally classified into two categories based on the electron configuration: (1) the light rare earth elements (LREEs), also termed as the cerium group, i.e., lanthanum to gadolinium (atomic numbers ranging from 57 to 64), and (2) the heavy rare earth elements (HREEs), e.g., terbium to lutetium (atomic numbers ranging from 65 to 71) (Gschneider, 1966).

Yttrium is grouped with the HREMs due to the similar ionic radius and chemical properties. The group is therefore called the yttrium group. Scandium is not classified into either LREEs group or HREEs group

Table 1. Characteristics of rare-earth metals (Zhang et al., 2016).

Element	Symbol	Atomic number	Atomic radii (Å)	RE ³⁺ radii ^a (Å)	Valence state	Electronic configuration	Abundance in upper earth's crust (ppm)
Lanthanum	La	57	1.877	1.061	+3	5d ¹ 6s ²	30
Cerium	Ce	58	1.825	1.034	+3,+4	4f ¹ 5d ¹ 6s ²	64
Praseodymium	Pr	59	1.828	1.013	+3,+4	4f ³ 6s ²	7.1
Neodymium	Nd	60	1.821	0.995	+3	4f ⁴ 6s ²	26
Promethium ^b	Pm	61	1.810	0.979	+3	4f ³ 6s ²	N/A
Samarium	Sm	62	1.802	0.964	+2, +3	4f ⁶ 6s ²	4.5
Europium	Eu	63	2.042	0.950	+2, +3	4f ⁷ 6s ²	0.88
Gadolinium	Gd	64	1.802	0.938	+3	4f ⁷ 5d ¹ 6s ²	3.8
Terbium	Tb	65	1.782	0.923	+3,+4	4f ⁹ 6s ²	0.64
Dysprosium	Dy	66	1.773	0.908	+3	4f ¹⁰ 6s ²	3.5
Holmium	Ho	67	1.776	0.894	+3	4f ¹¹ 6s ²	0.80
Erbium	Er	68	1.757	0.881	+3	4f ¹² 6s ²	2.3
Thulium	Tm	69	1.746	0.869	+3	4f ¹³ 6s ²	0.33
Ytterbium	Yb	70	1.94	0.859	+2, +3	4f ¹⁴ 6s ²	2.2
Lutetium	Lu	71	1.734	0.848	+3	4f ¹⁴ 5d ¹ 6s ²	0.32
Scandium	Sc	21	1.801	0.680	+3	3d ¹ 4s ²	13.6
Yttrium	Y	39	1.641	0.880	+3	4d ¹ 5s ²	22

^aRE³⁺ refers to trivalent rare-earth cations.

^bPromethium does not exist in nature.

because it has significantly different chemical properties, which are caused by smaller atomic and ionic radii (Zhang, Zhao, & Schreiner, 2016).

Table 1 illustrates the atomic number, atomic and ionic radii, valence state, electronic configuration and abundance in the upper earth's crust of REMs. Despite the fact that these elements are called "rare," the REMs are actually plentiful in the Earth's crust. The most abundant rare-earth metals, cerium, lanthanum, and yttrium, with the abundances (atom fraction) of 64, 30, and 22 ppm, respectively, have similar abundances as the common industrial metals such as nickel, copper, and lead. Thulium, the one having the least abundance among the RMEs, still has abundance approximately 200 times higher than gold.

The similarity of the physico-chemical properties of REMs is highly dependent upon their electronic configuration. Due to the similar energies of 5d and 4f electrons, there are two types of electronic configurations in lanthanide elements: 4fⁿ6s² and 4fⁿ⁻¹5d¹6s², with n = 1–14. The electronic configurations of lanthanum, cerium, gadolinium and lutetium belong to the 4fⁿ⁻¹5d¹6s² type, whereas other lanthanide elements have electronic configurations of the 4fⁿ6s² type. Although scandium and yttrium atoms do not consist of 4f electrons, their electronic configurations follow the type of ns²(n - 1)d¹ with n = 4 and 5, which is similar to lanthanum. This is the reason why they behave in a similar manner to other lanthanides. Thus, they are grouped into REMs. All the REMs can form M³⁺ ions due to the easy loss of electrons in ns²(n - 1)d¹ or 4f¹; some lanthanides can form the M²⁺ and M⁴⁺ ions. The states of +2 and +4 are generally less stable than the state of +3.

The REMs such as scandium, yttrium, lanthanum, gadolinium, and lutetium appear only as the M^{3+} ions due to the special stability of the inert gas configuration and the f^0 , f^7 , and f^{14} configuration. Similarly, the most stable M^{4+} can be formed for cerium and terbium because of the formation of the stable f^0 and f^7 configurations, respectively; europium and ytterbium can form the stable M^{2+} ions through achieving f^7 and f^{14} configurations, respectively. Especially, Ce(IV) is the only tetrapositive REM that is stable in both aqueous solution and solid compounds (Moeller & Ferrus, 1961). Ce(IV) can be simply obtained by reacting the Ce(III) salt solution with such strong oxidizing agents as ozone, hydrogen peroxide and peroxodisulfate. Due to its low toxicity and high redox potential, Ce(IV) can also be used as an effective oxidizing agent.

The electrons in the f orbital of lanthanides make them capable of having a wide range of coordination numbers (generally 6–12) (Cotton, 1994). Moreover, the coordination ability of lanthanide cation with ligands may increase with the decrease in the atomic/ionic radii. The “ionic” complex formed on the lanthanides is easily exchanged by other more electronegative ligands (Cotton, 2013). Based on the hard-soft acid-base consideration, the lanthanides have a higher affinity toward oxygen-containing ligands than other functional groups (Pearson, 1990).

3. Effective removal of arsenic by rare-earth metal based adsorbents

Adsorption is a process using solid materials with high surface areas, abundant functional groups and porous structure to remove contaminants from solution by chemical or physical forces (Gregg, Sing, & Salzberg, 1967). Compared to other technologies, adsorption is considered as one of the most promising approaches for arsenic removal due to its ease in operation, low material cost, high efficiency and good availability of adsorbents.

In recent decades, various adsorbents have been developed for the effective removal of arsenic species from water, including carbon-based materials, agricultural/industrial by-products, biological materials, and metal oxides. Among them, metal-based adsorbents are widely used because of their great availability from natural or artificial synthesis. The study on the arsenic removal using metal-based adsorbents was first reported in 1970s (Anderson, Ferguson, & Gavis, 1976). Since then, the adsorption behaviors and mechanisms of arsenic onto conventional metal-based adsorbents (e.g., iron, aluminum, and manganese) have been widely investigated (Babaeiveli, Khodadoust, & Bogdan, 2014; Giles, Mohapatra, Issa, Anand, & Singh, 2011).

In the past 10 years, the REM based adsorbents have attracted more attention due to their superior performance in eliminating arsenic respect

to the conventional ones. These innovative REM based adsorbents are mainly in the forms of metal oxide/hydroxide, metal oxide/hydroxide modified adsorbents, and metal ion impregnated adsorbents.

3.1. REM oxides/hydroxides

3.1.1. Single-species metal oxides/hydroxides

The REM oxides/hydroxides can be easily obtained by coprecipitation or hydrothermal methods. An abundant content of hydroxyl groups can be formed on the adsorbent surface during preparation, providing excellent performances for removal of arsenic and other anions such as fluoride and phosphate. The performances are highly affected by the solution pH. The adsorption capacities of different single REM oxides/hydroxides are summarized in Table 2.

Lanthanum is one of the least expensive and most abundant rare-earth elements and can be obtained from bastnesite and monazite (Sen & Peucker-Ehrenbrink, 2012). The performance of lanthanum compounds, including lanthanum hydroxide ($\text{La}(\text{OH})_3$), lanthanum carbonate ($\text{La}_2(\text{CO}_3)_3$), and basic lanthanum carbonate ($\text{La}(\text{OH})\text{CO}_3$), on the As(V) removal was first studied by Tokunaga, Wasay, & Park, (1997). The adsorption mechanism was suggested to be the ion exchange between the functional groups (e.g., $-\text{CO}_3$ and $-\text{OH}$) with As(V) ions in the neutral to alkaline pH range as described in Eqs. (1–3) and the formation of insoluble lanthanum arsenate (LaAsO_4) in the acidic pH range as expressed in Eq. (4).

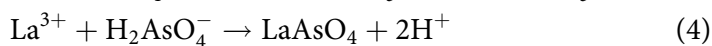
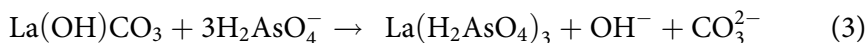
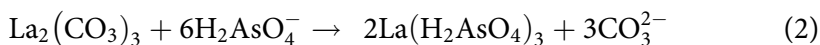


Table 2. Single rare-earth metal oxide/hydroxide adsorbents used for arsenic removal.

Adsorbent	Optimal pH	Isotherm model	Max. adsorption capacity (mg-As/g)		Ref.
			As(V)	As(III)	
Lanthanum hydroxide	3-8	–	–	–	(Tokunaga et al., 1997)
Lanthanum carbonate	4-7	–	–	–	
Basic lanthanum carbonate	2-4	–	–	–	
Hydrous cerium oxide	3 (As(V))	Langmuir (As(V))	107.1	171.88	(Li et al., 2012)
	7 (As(III))	Redlich Peterson (As(III))			
3D flower-like ceria composite	–	Langmuir	14.4	–	(Zhong et al., 2007)
Hydrated yttrium oxide	5	Langmuir	480.2	–	(Yu et al., 2016)
Yttrium hydroxide	4	Langmuir	289.6	–	(Lee et al., 2015)
Basic yttrium hydroxide	4	Langmuir	206.5	–	

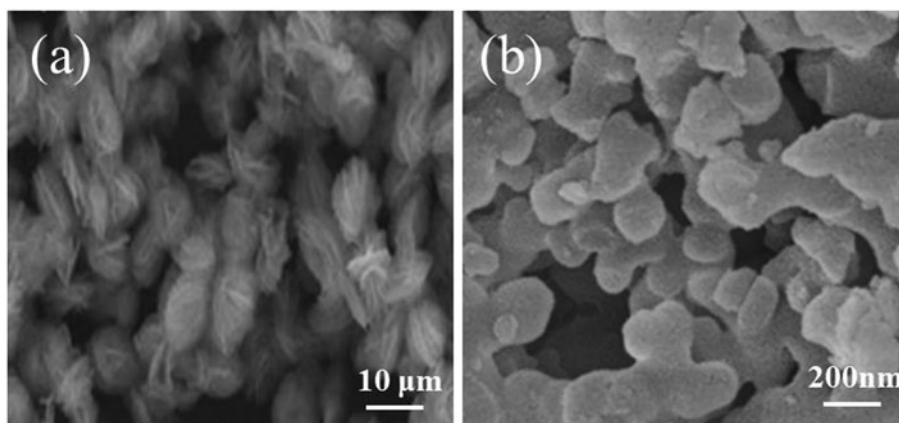


Figure 1. FESEM images of (a) 3-D flower-like ceria (Zhong et al., 2007) and (b) hydrous cerium oxide (Li et al., 2012).

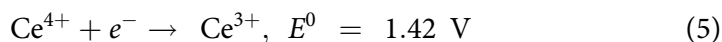
The growing interest on the use of cerium oxide for arsenic removal is due to its abundance, cost-effective and specific physico-chemical properties. Cerium oxide shows the highest stability in the acid among the REM oxides and has no leaching during the process of removing arsenic (Li, Li, Gao, & Shang, 2012). Ceria, with a 3-D flowerlike micro/nanocomposite structure, prepared through the ethylene glycol mediated process, was used as an effective adsorbent for arsenic removal (Zhong et al., 2007). As shown in Fig. 1(a), the ceria has a highly porous structure and high specific surface area, which result in a much higher uptake together with much faster kinetics when we compare it with the commercial ceria particles. More than 90% of the ultimate adsorption capacity was attained within 30 min. After the adsorption, the ceria can effectively be regenerated by a 0.2-M NaOH solution. However, the competitive adsorption performance of the 3-D ceria particles and the lanthanum compounds aforementioned toward other types of co-existing anions pollutants (e.g., phosphate and sulfate) with arsenic has yet to be studied in detailed, leaving a room for further research (Zhong et al., 2007).

A hydrous cerium oxide (HCO) nanoparticle with a specific surface area $198 \text{ m}^2/\text{g}$ and abundant surface hydroxyl groups was synthesized through a simple coprecipitation method (Li et al., 2012). As shown in Fig. 1(b), the HCO adsorbent was composed of porous aggregates with an average particle size of about 4 nm. The exceptional adsorption properties were observed on the adsorption capacity and kinetics of both As(V) and As(III). The adsorption capacities of HCO toward As(V) and As(III) at neutral pH reached more than 107 and 170 mg-As/g, respectively. Moreover, with the equilibrium arsenic concentration of $10 \mu\text{g}/\text{L}$ (the MCL for arsenic in drinking water regulated by the USEPA), the adsorption capacities of both As(V) and As(III) were over 13 mg-As/g, which were

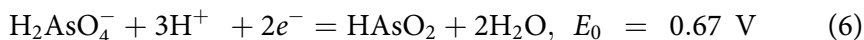
above most commercial adsorbents. A rapid adsorption was observed in the kinetics study with more than 80% of arsenic equilibrium adsorption achieved within 30 min. This exceptional arsenic adsorption performance by the HCO adsorbent resulted from the strong inner-sphere complexation based on the macroscopic and microscopic analysis.

The HCO adsorbent had demonstrated its good potential in industrial-scale treatment of by the 65- $\mu\text{g/L}$ arsenic-contaminated natural water. Nearly 100% removal of arsenic was achieved with a low HCO adsorbent loading; the adsorption performance was improved with an increase in ion strength, suggesting that it was also suitable for the applications in the wastewater treatment (Li et al., 2012).

In addition to having higher content of hydroxyl groups, the cerium oxide has Ce(IV), which can potentially oxidize As(III) in water due to its high redox potential. The redox activity of cerium oxide is reportedly dependent upon the ratio of $\text{Ce}^{4+}/\text{Ce}^{3+}$ on the adsorbent surfaces, which is highly affected by such synthesis parameters as temperature and medium pH (Gupta, Das, Neal, & Seal, 2016). The redox potential of $\text{Ce}^{4+}/\text{Ce}^{3+}$ is as below (Paulenova, Creager, Navratil, & Wei, 2002):



The predominant species of As(V) and As(III) at neutral pH are $\text{H}_2\text{AsO}_4^{-}$ and $\text{H}_3\text{AsO}_3/\text{HAsO}_2$, respectively. The redox reaction and the potential of As(V)/As(III) are as follows (Lee & Choi, 2002). Accordingly, the redox reaction between As(III) and Ce(IV) oxide is favorable.



The Ce(IV) oxide can be prepared by using a variety of cerium salts such as those containing Ce^{4+} or Ce^{3+} as well as elemental cerium metal (Zhou & Rahaman, 1993; Hirano & Kato, 1996; Inoue, Kimura, & Inui, 1999; Sun, Li, Zhang, Wang, & Chen, 2005). It is suggested that Ce^{3+} salts can be simply oxidized to Ce^{4+} by adding oxidant reagents such as peroxyacetic acid (Chen, Xu, Song, Xu, Ding, & Sun, 2008). Even in an atmospheric environment, partial oxidation of Ce^{3+} may be caused by aerial oxygen, leading to the presence of mixed valent cerium on the cerium oxide prepared solvothermally in ethanol from $\text{CeCl}_3 \cdot 7\text{H}_2\text{O}$ (Zhang, Jin, & Chan, 2004).

Ce^{3+} can partially be oxidized by aerial oxygen at 300 °C after being sprayed by a heated substrate (Jennifer, Drobek, Rossi, & Gauckler, 2007). Although the precipitation method works well for the preparation of cerium oxide under an ambient conditions the hydrothermal/solvothermal reactions allow better control over crystal growth in terms of particle size and shape.

The particles prepared by a conventional precipitation were found to be consisted of aggregates of CeO_2 (Taniguchi, Watanabe, Sakamoto, Matsushita, & Yoshimura, 2008). On the other hand, the hydrothermal/solvothermal reactions can well control the degree of crystal formed by appropriate selection of suitable solvent, additives, and reaction temperature. As shown in Fig. 2, the average particle size of CeO_2 crystals is obviously affected by the reaction temperature.

The specific surface area of ceria microspheres synthesized in benzyl alcohol was reportedly twice higher than that of 3-D flower-like ceria synthesized in ethylene glycol, leading to a better removal capacity (Xiao, Ai, & Zhang, 2009). The physico-chemical properties of cerium oxide nanoparticles (e.g., dispersion stability, particle size, and oxidization potential) can be significantly affected by the type of precursor Ce^{3+} salts (Barkam et al., 2017). A higher Ce^{4+} content in the particle surface was observed when cerium sulfate was employed as a precursor salt. Different crystal forms of CeO_2 nanoparticles, such as single-crystalline and monodispersed cubic nanoparticles, nanorods, and nanocubes, can be hydrothermally synthesized simply by adjusting the concentrations of NaOH and $\text{Ce}(\text{NO}_3)_3$ (Sakthivel et al., 2013). Therefore, cerium oxide can be well designed by controlling the conditions in the preparation process and applied as functionalized adsorbents for the simultaneous oxidation and adsorption of arsenic from natural water and groundwater without having additional oxidation process.

Highly active hydrated yttrium oxide (HYO) with great affinity toward As(V) was recently developed through a one-step hydrothermal process (Yu et al., 2016). The HYO adsorbent exhibited an excellent adsorption performance of As(V) in a wide pH range of 4.0–7.0. The maximum adsorption capacity of HYO reached 480.2 mg-As/g at pH 5.0. Based on both kinetics and isotherm studies, the adsorption of As(V) was shown to be a monolayer chemical adsorption process; the ion exchange between the hydroxyl groups on the HYO adsorbent and As(V) ions took place and As(V) anions were bonded to the yttrium oxide via the linkage of As-O-Y.

Although hydrated yttrium oxide had an exceptional adsorption capacity toward arsenic, the existence of other anions such as phosphate and fluoride greatly hindered the arsenic uptake due to extensive competition between these anions and arsenic. Despite of such problems, the adsorption capacity of this adsorbent was still higher than many reported adsorbents. Therefore, the HYO can be applied for simultaneous removal of arsenic and fluoride or phosphate from the real wastewater with only being slightly affected by natural organic matter and other anions (Yu et al., 2016).

Lee and coworkers (2015) used yttrium hydroxide ($\text{Y}(\text{OH})_3$) and basic yttrium carbonate ($\text{Y}(\text{OH})\text{CO}_3$) for the removal of arsenic from water. The maximum adsorption capacities of $\text{Y}(\text{OH})_3$ and $\text{Y}(\text{OH})\text{CO}_3$ for As(V) were

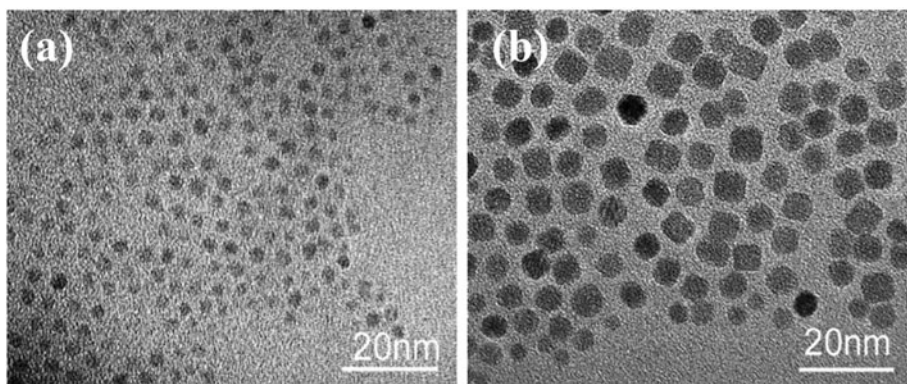


Figure 2. TEM images of the CeO₂ nanoparticles hydrothermally synthesized at different temperature for 6 h: (a) 150 °C and (b) 200 °C (Taniguchi et al., 2008b).

respectively 206.5 and 289.6 mg-As/g at pH 7. It was found that the ion exchange between carbonate and arsenic, and coprecipitation were the mechanisms for the arsenic uptake. However, these two adsorbents were less stable at acidic conditions based on the results from the TEM analysis. The adsorption performance of yttrium-based adsorbents was greatly influenced by the existence of phosphate ions. In order to improve the stability in acidic condition, the Y(OH)₃ nanoparticles were further be transformed to Y₂O₃ nanoparticles by the calcination process at 450 °C (Fang et al., 2003). However, it was found that the loss of surface hydroxyl groups during the calcination process significantly reduced the adsorption capacity of the adsorbent toward arsenic.

The regeneration study of these single-species REM oxides/hydroxides is not extensively studied, which is crucial for the real-world applications. Although it was demonstrated that these adsorbents could be regenerated (Zhong et al., 2007; Lee et al., 2015), the adsorption capacity toward arsenic reduced significantly in the subsequent cycles. This indicates that these REM adsorbents may be not suitable for long-term industrial-scale applications, as the regeneration and reuse of spent adsorbents are of great importance. The poor adsorption performance of the regenerated adsorbents in the next cycles can be due to the instability of adsorbents, because the structures of adsorbents were destroyed by the strong acids or bases used in the regeneration. Further study aiming to improve the reusability of these adsorbents is required to explore their potentials in the water treatment.

3.1.2. Multiple-species REM oxides/hydroxides

The current price of powder lanthanum or cerium salts (>99.5%) is around US \$8,000–10,000/ton. Due to the relatively high cost of REMs, it is wise to use the REMs, and well available and less costly metals (e.g., iron and

manganese) to fabricate a new series of composites as adsorbents in order that the benefits of REMs can be kept while the overall cost can be reduced.

Moreover, such work further reportedly improves the uptake performance of arsenic (Zhang, Yang, Dou, He, & Wang, 2005). For example, the incorporation of iron oxides with ceria (CeO_2) was able to improve the adsorption of arsenic due to the relatively small ionic radius and the abundant hydroxyl groups on the surfaces of CeO_2 (Chen, Zhu, Guo, Qiu, & Zhao, 2013). It was demonstrated that a granular iron oxide doped with the ceria had a high efficiency in removing arsenic from the real arsenic-contaminated groundwater; the MCL of arsenic could be achieved in a long-term operation for 4 months (Zhang et al., 2005). Besides, this metal oxide can be regenerated and used for at least five cycles and 70% of the initial adsorption capacity can be retained (Chen et al., 2013).

Several naturally occurring and powder-typed REM oxides from Southern India with the chemical compositions of La_2O_3 (44.0%), Nd_2O_3 (36.5%), Pr_6O_{11} (10.5%), Sm_2O_3 (5.0%), and CeO_2 (2.0%) were used for the As(V) removal, reported by Raichur and Panvekar (2002). The mixed rare-earth oxides showed rapid adsorption kinetics; more than 90% of arsenic uptake were accomplished within the first 10 min. The presence of phosphate seemed to have less influence on the adsorption of arsenic than sulfate, nitrate and silicate due to the existence of different types of adsorption sites on the mixed oxides. Furthermore, the mixed REM oxides showed fast desorption at basic pH, but the exact reusability of these oxides is unknown as the adsorption capacity in the subsequent cycles was not provided.

Zhang and coworkers (2003) synthesized a nanostructured Ce(IV)-doped iron oxide adsorbent by a coprecipitation method; the adsorbent showed constant adsorption over a wide pH range of 3–7, with the maximum adsorption capacity of 70.4 mg-As/g at pH 5. The presence of phosphate significantly inhibited the As(V) removal. On the other hand, such factors as salinity, hardness, and existence of other anions (Cl^- , F^- , NO_3^- , and SO_4^{2-}) had no distinct impact.

The same group of researchers further investigated the role of surface properties of Fe-Ce bimetal oxide adsorbent on the As(V) adsorption (Zhang et al., 2005). In the adsorption experiments, the multiple-species metal oxides exhibited a much better As(V) adsorption capacity than the single-species metal oxides (CeO_2 and Fe_3O_4) prepared by the same methods and other previously reported adsorbents. This may be due to the fact that more hydroxyl groups (30.8%) exist on the bimetal oxide adsorbent than CeO_2 and Fe_3O_4 (12.6% and 19.6%) respectively, according to the FTIR and XPS studies. Meanwhile, the integral area of the As-O band at

836 cm^{-1} (from the FTIR analysis) had a linear relationship with the As(V) adsorption capacity. Concurrently the decrease in the integral area of M-OH band at 1126 cm^{-1} suggests that the adsorption of arsenic on Fe-Ce adsorbent primarily occurred through the ligand exchange mechanism (Zhang et al., 2005). The existence of coexistent fluoride (F) and phosphate (P) might have a certain influence on the As(V) adsorption. The XPS analysis demonstrated that As(V) and P were generally adsorbed through the replacement of iron surface active sites, while F was mostly adsorbed through the exchange of Ce surface active sites (Zhang et al., 2010). The As *k*-edge spectra according to the extended X-ray absorption fine structure spectroscopy (EXAFS) showed that the second peak of Fe-Ce was attributed to As-Fe shell after adsorption of As(V); this further supports that arsenic adsorption mainly occurs on the iron surface active sites.

Other different types and structures of Fe-Ce mixed oxides were also reported for the arsenic removal from water (Zhang et al., 2010; Basu & Ghosh, 2013; Chen et al., 2013; Chen et al., 2014a, 2014b; Sahu, Sahu, Mohapatra, & Patel, 2016). As shown in Fig. 3, hollow iron-cerium alkoxides and ordered mesoporous cerium-iron mixed oxide were synthesized by the hydrothermal and nanocasting methods, respectively (Chen et al., 2014a, 2014b). The hollow cerium alkoxides had high arsenic uptake; however, the coexisting anions such as phosphate and silicate significantly influenced the removal efficiency of arsenic. On the other hand, the ordered mesoporous cerium-iron mixed oxide can be regenerated with high desorption efficiency and slight loss of adsorption capacity in five consecutive cycles. Compared to the composite formed by precipitation, using hydrothermal method and casting template can obtain highly ordered porous composites with relatively larger surface area and pore volume (Jiao, Harrison, Jumas, Chadwick, Kockelmann, & Bruce, 2006). Similarly, the ligand exchange between arsenic species and other negatively charged groups on the adsorbent surface was proposed to be the main adsorption mechanism as listed in Table 3.

A Ce(IV)-Al(III) binary oxide with the particle sizes in the range of 8–10 nm was synthesized through a one-step hydrothermal reaction (Bhattacharya, Gupta, & Ghosh, 2017). The adsorption performance of the composite remained unchanged at $\text{pH} < 9$ and slightly reduced at $\text{pH} > 9$. The adsorption process followed the pseudo-second-order kinetics equation and the Langmuir isotherm with the maximum adsorption capacity of 21 mg-As/g. It has to be pointed out that the reusability of the binary oxide and impacts of other anions in water on the adsorption were not investigated, leaving a room for further studies.

Chong and coworkers (2009) prepared a Ce(IV)-La(III) binary hydroxide adsorbent from a waste ceria powder via a method that combined with

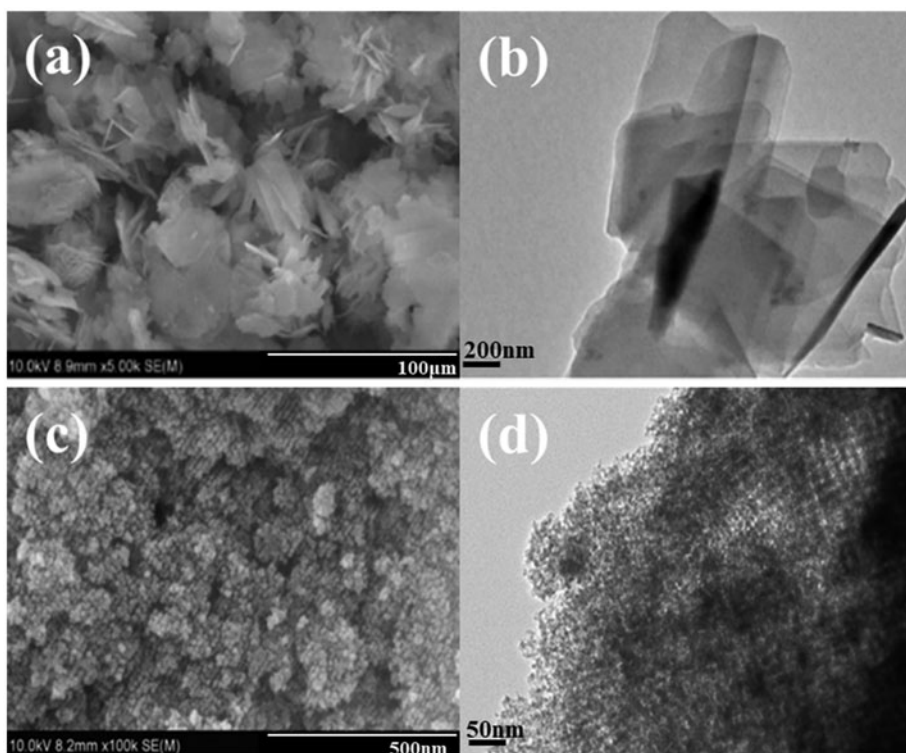


Figure 3. FESEM (a) and TEM (b) images of hollow iron-cerium alkoxides (Chen et al., 2014a); FESEM (c) and TEM (d) images of ordered mesoporous cerium-iron mixed oxide (Chen et al., 2014b).

acid and heating treatment. The waste ceria powder with the composition of 51% CeO_2 and 32% La_2O_3 was firstly dissolved by 2-M H_2SO_4 ; the mixture was then completely precipitated by adding a NaOH solution, by which the adsorbent was formed. The maximum adsorption capacities of the mixed hydroxide adsorbent toward As(V) and As(III) were 89.9 and 84.1 mg-As/g, respectively.

The adsorption capacities for arsenic ions were remained unchanged, when the drying operation was performed below 100°C ; the adsorption capacity decreased gradually with the further increase in the drying temperature. This may be due to the loss of hydroxyl groups on the adsorbent surface caused by the high drying temperature. Since the concentrations of cerium and lanthanum in the finishing solution were found to be undetectable at the pH range of 4–11, the arsenic adsorption was principally attributed to the formation of inner-sphere complexes rather than precipitation of an Ce(IV)/La(III) arsenate or Ce(IV)/La(III) arsenite.

The Ce(III) -doped titanium oxide for the arsenic uptake was prepared through a precipitation and hydrolysis-precipitation method (Deng, Li, Huang, & Yu, 2010; Li, Deng, Yu, Huang, & Lim, 2010). The amorphous

Table 3. Mixed oxide/hydroxide adsorbents containing rare-earth metals used for arsenic removal

Adsorbent	Optimal pH	Isotherm model	Max. adsorption capacity (mg-As/g) ^a		Mechanism	Ref.
			As(V)	As(III)		
Natural mixed metals	6.5	Langmuir	2.945	–	–	(Raichur and Panvekar, 2002)
Cu/Mg/Fe/La layered double hydroxide	6	Langmuir	43.5	–	Ligand exchange of -OH and CO ₃ ²⁻	(Guo et al., 2012)
Ce(IV)-doped iron oxide	5	Langmuir	70.4	–	Ligand exchange of -OH (major role) and SO ₄ ²⁻ groups	(Zhang et al., 2003)
Nanostructured Fe(III)-Ce(IV) oxide	7	–	–	–	–	(Basu and Ghosh, 2013)
Ordered mesoporous Ce(IV)-Fe(III) oxide	4	Freundlich ^a /Langmuir ^b	106.21	75.36	Electrostatic interaction/Ligand exchange of -OH groups	(Chen et al., 2014a)
Mesoporous Ce-Fe oxide	5.5	Langmuir	91.74	–	Replacement of -OH groups	(Chen et al., 2013)
Hollow Fe(III)-Ce(III) alkoxides	6	Freundlich ^a /Langmuir ^b	206.6	266.0	Ion-exchange of -OH, CO ₃ ²⁻ and unidentate carbonate-like species	(Chen et al., 2014b)
Ce(IV)-La(III) binary hydroxide	7	–	89.9	84.1	Electrostatic interaction/Inner-sphere complexes	(Chong et al., 2009)
Ce(III)-doped titanium dioxide	6	Langmuir	44.9	55.3	Electrostatic interaction/Surface complexes	(Deng et al., 2010; Li et al., 2010)
Ce(IV)-doped titanium dioxide	6.5	Freundlich ^a /Langmuir ^b	24.41	–	Involvement of -OH groups	(Jomekian et al., 2011)
Ce(IV)-incorporated manganese oxide	7	Freundlich	18.653	–	Replacement of -OH groups	(Gupta et al., 2011)
Y(III)-Al(III) binary oxide	6.6	Langmuir	62.23	–	Electrostatic interaction/Involvement of -OH groups	(Zhang et al., 2012)
Y(III)-Mn(II,III,IV) binary oxide	7	Langmuir	279.9	–	Electrostatic interaction/Involvement of -OH groups	(Yu et al., 2015)
Ti-loaded basic yttrium carbonate	7	Langmuir	348.5	–	Ion exchange of carbonate groups	(Lee et al., 2015)
La-impregnated titanium oxide	5	Langmuir	114	–	Electrostatic interaction/Surface complexes	(Yan et al., 2016)
Ce(IV)-Al(III) binary oxide	5	Langmuir	21	–	–	(Bhattacharya et al., 2017)

^aIsotherm for arsenite (As(III)) removal.^bIsotherm for arsenate (As(V)) removal.

and porous Ce-Ti hybrid adsorbents were collected in the form of nanoparticles with the sizes in the ranges of 100 to 200 nm. The hybrid adsorbent had much higher adsorption capacity than both pure titanium oxide and cerium oxide, mainly due to its amorphous compositions and the nano-scale components. The spent adsorbent could be effectively regenerated using 0.5-M NaOH, and about 80% of adsorption capacity remained after five cycles of adsorption-desorption process (Li et al., 2010). Besides that, the hybrid adsorbent was applied in a down-flow column test, where a simulated arsenic-contaminated groundwater was used as the influent. Approximately 6500 bed volumes of arsenic solution can be effectively treated in the presence of competitive anions (Deng et al., 2010). After the adsorption, the peak assigned to hydroxyl groups on metal oxides (M-OH) decreased; this suggests that the M-OH groups on the adsorbent surface are involved in the arsenic removal. As illustrated in Fig. 4, the adsorption of As(V) was controlled by a combined mechanism of electrostatic interaction and formation of monodentate and bidentate surface complexes, while neutral As(III) can be only adsorbed via the formation of monodentate complexes (Li et al., 2010).

Jomekian and coworkers (2011) studied the adsorption performance of Ce-Ti adsorbent toward As(V) anions. It was found that the microstructure of the adsorbent and the amount of hydroxyl groups on the adsorbent surface were highly affected by the cerium valence. The Ce(III) doping resulted in a higher micropore surface area and volume than the Ce(IV) doping, and the adsorption capacity of Ce(III)-doping titanium oxide was nearly double times higher than that of Ce(III)-doping ones.

A nanostructured Ce-incorporated manganese oxide was prepared by a coprecipitation-calcination and sol-gel method (Gupta et al., 2011). An excellent efficiency of arsenic removal was demonstrated. The adsorption reaction is chemisorption type and the replacement of hydroxyl groups by arsenic species occurs as follows.



The yttrium based composite materials have recently attracted increasing attentions. Yu et al. (2015) reported that a yttrium-manganese binary oxide prepared by a one-step coprecipitation method had an extremely high adsorption capacity of 279.9 mg-As/g for As(V) at pH 7. The composite adsorbent had loose structure and composed of nano-sized flakes. The adsorption experimental data were well fitted by the pseudo-second-order kinetics equation and the Langmuir isotherm. A much higher affinity for As(V) than for As(III) was observed in the whole pH range being tested; this suggests that the oxidation of As(III) is unlikely to occur. The adsorbent was stable in both neutral and alkaline conditions; however a slight

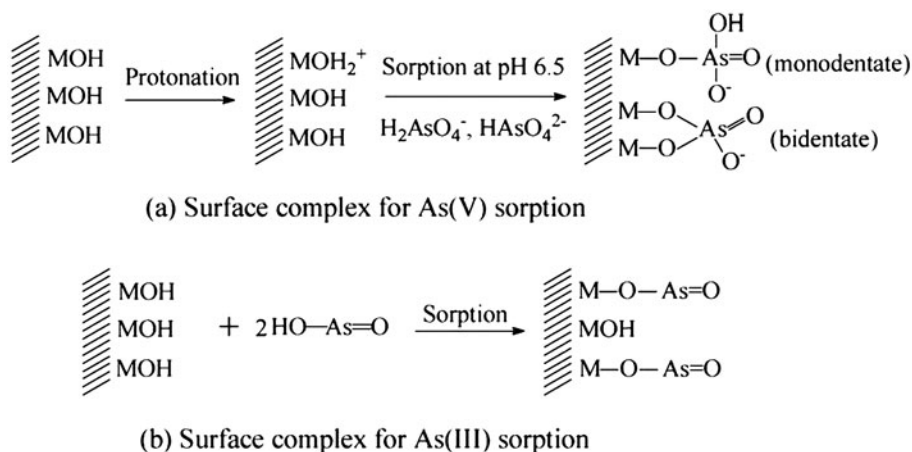


Figure 4. Schematic diagram for the possible complexes for As(V) and As(III) formed on Ce-Ti adsorbent (Li et al., 2010).

dissolution was observed in a stronger acidic condition. A high adsorption capacity (above 220 mg-As/g) toward arsenic can be maintained even in the presence of several strongly competitive anions in the solution. In contrast, the mesoporous yttrium-aluminum adsorbent developed by an incipient wetness impregnation method can reportedly function well over a relatively narrower pH range, with the maximum uptake of 62.23 mg-As(V)/g at pH 6.6 (Zhang, Xu, Zhang, Zhang, & Xu, 2012).

Until now, a Ti-loaded basic yttrium carbonate showed the highest adsorption capacity (348.5 mg-As/g) for As(V) at pH 7 and retained the highest adsorption capacity with the presence of coexisting anions compared to other reported adsorbents (Lee et al., 2015). This adsorbent had a higher adsorption rate than virgin basic yttrium carbonate and yttrium hydroxide. However, it was limited to two cycles of adsorption operation due to the poor regenerated adsorption capacity. This could restraint it from large-scale applications in water treatment.

The La-impregnated titanium dioxide composite was studied on its adsorption properties and mechanism in the simultaneous removal of arsenic and fluoride (Yan, Tu, Chan, & Jing, 2017). The orientated lanthanum oxide was grown on the faceted TiO_2 , resulting in 23.7 m^2/g of specific surface area and average pore size of 38 nm. The adsorption process was found to be well fitted by the Langmuir isotherm and the pseudo-second-order kinetics equation, with the maximum adsorption capacity of 114 mg-As(III)/g at pH 5. The higher adsorption capacity of this composite toward As(III) than fluoride was due to the fact that two sites (La and Ti mixed sites) were available for As(III) uptake while only one site (La) was for the fluoride adsorption. The increasing fluoride concentration in the solution significantly retarded the arsenic adsorption by the steric hindrance imposed by adsorbed fluoride ions on the La sites for the access of

As(III). Furthermore, As(III) formed monodentate configuration on La sites while bidentate configuration on Ti sites based on the EXAFS result (Yan et al., 2016). At high pH, As(III) was more favorable to be adsorbed on the La sites than Ti sites.

3.2. REM oxide/hydroxide modified adsorbents

Several supporters for adsorptive materials such as clays, porous silicon materials, carbon materials and organic polymer composites are reported for loading metal oxides/hydroxides. The uniform distribution of the loaded metal oxides/hydroxides on the surface of supporting materials should be advantageous for the diffusion of arsenic species to all the active sites (Hui, Zhang, & Ye, 2015; Cheng et al., 2016).

Additionally, the metal oxides/hydroxides may easily aggregate into large particles under continuous stirring while using these matrix materials to disperse metal oxides/hydroxides would be great to overcome this drawback. The loaded metal oxides/hydroxides provide the most adsorptive sites for the arsenic removal. The working mechanism of metal oxide/hydroxide modified adsorbents is therefore similar to that of pure metal oxide/hydroxide, while the properties of supports may also affect the performance of the resulting adsorbents. The synthesis methods and arsenic removal performance of previously reported metal oxide/hydroxide modified adsorbents are summarized as follows, according to the types of supporting materials, with their working performance illustrated in Table 4.

Montmorillonites (clay materials) are widely used as the adsorbents due to their high abundance in nature, good chemical and mechanical stability, excellent ion-exchange capacity, high specific surface area, and low cost (Bailey, Olin, Bricka, & Adrian, 1999; Bhattacharyya & Gupta, 2008; Krishna, Murty, & Prakash, 2000; Lin & Juang, 2002). They are comprised of units built of a central alumina octahedral sheet with two silica tetrahedral sheets. A negative charge is generated on the two large surfaces of montmorillonite unit by the isomorphous substitution of Mg^{2+} and Fe^{2+} for Al^{3+} in octahedral sheet or Al^{3+} for Si^{4+} in tetrahedral sheet. This negative charge is neutralized by interlayer cations (e.g., Na^+), which can easily be exchanged by other cations or molecules (Pramanik, Srivastava, Samantaray, & Bhowmick, 2001).

The REM oxide/hydroxide modified montmorillonite can be synthesized by simply mixing metal ions and sodium montmorillonite under vigorous stirring, followed by adding a certain amount of sodium hydroxide. Wang and coworkers (2015) synthesized a Fe/La-modified montmorillonite (Fe/La-Mt) with a surface area of $167.40\text{ m}^2/\text{g}$ and a total pore volume of $0.152\text{ cm}^3/\text{g}$. The adsorption of roxarsone onto the adsorbent can be well

Table 4. Rare-earth metal oxide/hydroxide modified adsorbents used for arsenic removal.

Adsorbent	Optimal pH	Isotherm model	Max. adsorption capacity (mg-As/g)		Ref.
			As(V)	As(III)	
Clay + Ce(OH) _n	6	Langmuir	5.1	5.2	(Seida & Izumi, 2005)
Clay + Ce→OH			11.9	12.1	
Lanthanum-loaded zeolite ^a	5	–	18.8	–	(Pu, Huang, & Jiang, 2008)
Lanthanum-impregnated SBA-15	7.2	Langmuir	126.7	–	(Jang et al., 2004)
CeO ₂ -loaded silica monoliths ^b	–	–	6.84	7.0	(Sun et al., 2012)
Hydrous cerium oxide-graphene	7	Langmuir	41.31	–	(Yu et al., 2015)
CeO ₂ -CNTs	3.1	Freundlich	–	–	(Peng et al., 2005)
Y(OH) ₃ -coated cellulose fiber	5-7	–	–	–	(An et al., 2012)
Ce-modified chitosan nanobioadsorbent	8	Langmuir	–	57.5	(Zhang et al., 2016)
ZnO:CeO ₂ :nanocellulose: polyaniline bio-composite	8	Freundlich and Dubinin-Radushkevich	–	–	(Nath et al., 2016)
Ceria-GO	–	Langmuir	212	185	(Sakthivel et al., 2017)
Ce-loaded volcanic rocks	<9	Freundlich and Dubinin-Radushkevich	0.255 (Ce-Rs) 0.893 (Ce-Pu)	0.643 (Ce-Rs) 1.974 (Ce-Pu)	(Asere et al., 2017)
PAC-CeO ₂	6 (As(III)) 8 (As(V))	Freundlich	12	12	(Sawana et al., 2017)
Cerium oxide modified activated carbon	5	Langmuir	43.60	36.77	(Yu et al., 2017)

^aAdsorption capacity was estimated from the removal efficiency of arsenic under different adsorbent dosages.

^bAdsorption capacity was obtained at the initial arsenic concentration of ~100 µg/L.

described by the pseudo-second-order kinetics equation and the Langmuir isotherm, with a maximum adsorption capacity of 32.82 mg-As/g at the room temperature.

The insoluble clay + Ce(OH)_n conjugates and clay + Ce→OH conjugates were respectively synthesized by electrostatically immobilizing cerium hydroxide in the inner layers of highly dispersed Na-montmorillonite (clay) and by incorporating the clay with active cerium ions followed by the hydrolysis (Seida & Izumi, 2005). It was found that the adsorption capacity of the clay + Ce→OH conjugates was much higher than that of clay + Ce(OH)_n conjugates. This is probably due to the fact that the clay + Ce→OH conjugates had higher surface area and mesopore volume, and better dispersion of cerium hydroxide than clay + Ce(OH)_n conjugates. The formation of stable inner-sphere bidentate bimolecular complexes on the surfaces of cerium hydroxides was responsible for the strong adsorption of arsenic. The adsorption performance of the clay incorporated cerium conjugates was slightly affected by the coexisting anions, where more than 90% of arsenic can be removed. The clay support could possibly restrain the other anions from the active sites and thus the good removal efficiency of arsenic was maintained. This

indicates that this adsorbent can be used in the real wastewater treatment, where the coexisting anions exist.

There is a growing interest in the use of zeolite, because of its specific properties such as high surface area, sieving and ion exchangeable properties, high abundance and low cost (Breck, 1974; Lin & Juang, 2009). Zeolites are composed of a framework of alumina-silicates with a three-dimensional structure of SiO_4 and AlO_4 tetrahedral molecules bonded to each other by sharing oxygen atom (Kesraoui-Ouki, Cheeseman, & Perry, 1994). The partial substitution of tetravalent Si by trivalent Al or Fe ions gives the zeolite frameworks negatively charged sites that are normally neutralized by cations such as Na^+ , Mg^{2+} , and Ca^{2+} . These electrostatically attracted cations in the zeolites can be easily exchanged by other heavy metal ions. The lanthanum-loaded zeolite with the properties of good availability, excellent adsorption capacity and wide optimum pH range was applied for the As(V) removal (Pu et al., 2008). The spent adsorbent could be successfully regenerated with 1-M NaOH. The uptake of arsenic is due to a combined process of the ion exchange of hydroxyl groups and electrostatic adsorption of negative charged As(V) anions on the positive charged lanthanum oxide.

The well-ordered mesoporous silica materials are of increasing importance for their properties: tunable pore size, high specific surface area, large pore volume, and rich morphology (Wu, Mou, & Lin, 2013). These materials incorporated with the metals were reported, which has the catalytic activity for the specific uses (Ou et al., 2007).

As shown in Fig. 5(a), Santa Barbara Amorphous (SBA-15), with well-ordered hexagonal nano-sized pore arrays of uniform pore size, was synthesized under acidic condition in the presence of nonionic triblock copolymer P123 as a template (Chen, Do & Gu, 2009; Vinu, Murugesan, & Hartmann, 2004; Wu et al., 2013). Jang and coworkers (2004) successfully synthesized the lanthanum oxide-incorporated SBA-15 (LaSBA-15) for the As(V) removal. The most efficient As(V) removal was achieved by 50% lanthanum-impregnated SBA-15 by weight, with the maximum capacity of 126.7 mg-As/g. It was found that at 80% lanthanum impregnation, unrestrained substitution of lanthanum in the silica network took place, leading to an overall reduction in the As(V) uptake, even though the dispersion of nano-scale lanthanum oxide was homogeneous in the mesoporous structure of SBA-15. Due to the fact that most active sites on the lanthanum oxide were distributed in the relatively uniform hexagonal-open mesopore of the SBA-15, the impregnation of nano-size lanthanum oxide onto the SBA-15 resulted in improvement of adsorption rate and capacity and reduction of cost for arsenic removal.

The mesoporous silica monolith with micro-sized pores was used for loading hydrous cerium oxide (CeO_2) nanoparticles and applied for arsenic

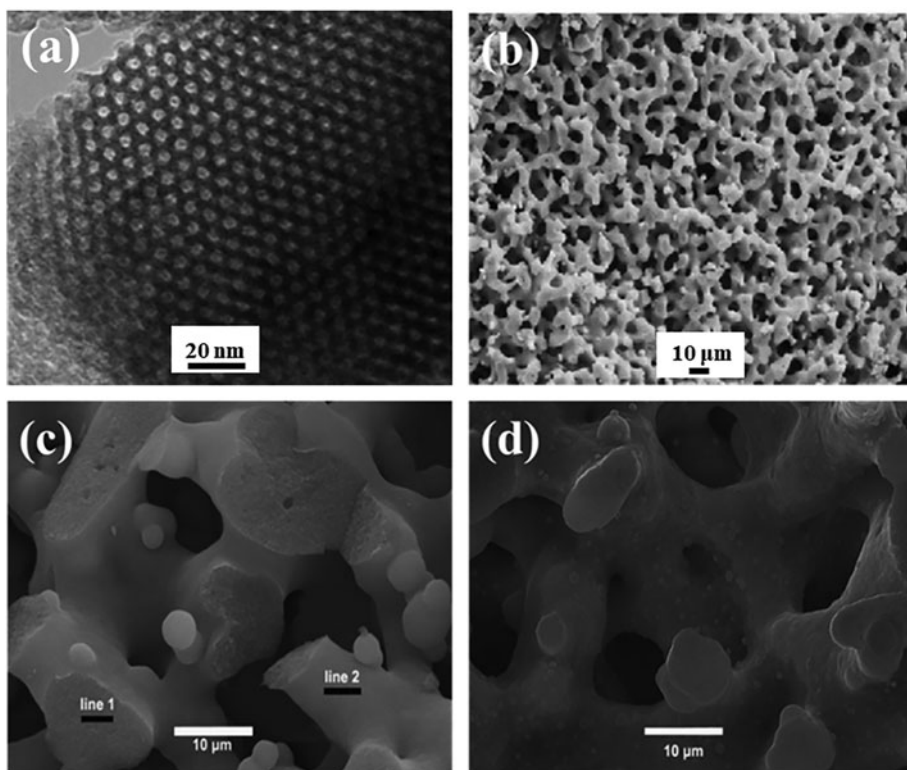


Figure 5. Structure of mesoporous silica materials: (a) TEM image of virgin SBA-15 (Xing et al., 2018); (b) FESEM image of virgin silica monoliths, (c) FESEM high-resolution image of virgin silica monoliths, and (d) FESEM high-resolution image of CeO_2 -loaded silica monoliths (Sun et al., 2012).

adsorption in a dynamic flow through reactor (Sun, Li, Gao, & Shang, 2012). As shown in Figs. 5(b) and (d), 3-dimensional interconnected macropores in silica monoliths were advantageous for the uniform attachment of CeO_2 nanoparticles on the silica skeleton and the effective mass transfer of arsenic ions to the active adsorption sites. At a small empty bed contact time of 4 min, the breakthrough bed volume of 20,000 could be achieved for treating the arsenic-containing natural water of $\sim 80 \mu\text{g/L}$ to meet the MCL of arsenic for drinking water. After being treated by using 1% H_2O_2 solution at pH 11, the composite still had its strong arsenic adsorption performance, which is of great importance for their potential industrial applications.

Novel carbon materials such as graphene and carbon nanotubes (CNTs) have attracted growing attention recently due to their exceptional properties and potential applications (Gojny, Wichmann, Fiedler, Bauhofer, & Schulte, 2005; Xu, Yang, Wang, Zhou, & Shen, 2012; Zhang, Zhang, Wang, & Liu, 2004; Zhu et al., 2010). Because of their high specific surface area, and great thermal and chemical stability, many metal oxides/hydroxides

were reportedly coated on the surface of graphene and CNTs (Planeix et al., 1994; Li et al., 2002; Wu et al., 2012; Yin et al., 2013).

Peng et al. (2005) developed ceria supported on carbon nanotubes (CeO₂-CNTs) for As(V) removal through a simple precipitation-calcination method. The ceria particles with a particle size of about 6 nm could be homogeneously distributed on the surface of CNTs, leading to an increase in the specific surface area from 153 to 189 m²/g. The adsorption was found to be pH-dependent. The presence of 10 mg/L Ca²⁺ and Mg²⁺ in solution significantly enhanced the adsorption capacity of the CeO₂-CNTs from 10 to 81.9 and 78.8 mg-As/g, respectively. The increased adsorption capacity with the existence of Ca²⁺ and Mg²⁺ in the solution was possibly due to the ternary surface complex reactions. The cations first exchanged with the hydrogen from the surface groups and then As(V) anions were adsorbed by forming the surface complexes such as -Ce-O-Ca(Mg)-As(V). This hybrid material was able to be regenerated easily with a dilute NaOH solution.

A high-performance hydrous cerium oxide modified graphene (GNP-HCO) was synthesized by a facile wet-chemistry route for arsenic removal (Yu, Ma, Ong, Xie, & Liu, 2015). An extremely rapid adsorption rate was observed; above 88% of the equilibrium adsorption capacity of As(V) was completed within the initial 20 min. Such good performance in the adsorption kinetics is due to the high activity of hydrous cerium oxide and large surface area of graphene. As shown in Figs. 6(a) and (b), the TEM analysis showed that the transparent graphene sheet was randomly decorated by the dark-colour cerium oxide particles with a size of ~10 nm. The adsorption can be well described by the pseudo-second-order kinetics equation and the Langmuir isotherm, indicating that chemisorption process occurred. The maximum adsorption capacities were 62.33 and 41.31 mg-As/g at pH 4.0 and 7.0, respectively, higher than most modified carbon-based adsorbents previously reported. The adsorption capacity of GNP-HCO was significantly reduced in the presence of phosphate; however, it was only slightly affected by such anions as fluoride, carbonate, and sulfate. The material showed its potential industrial applications for reduction of the arsenic to meet the regulated level of below the MCL.

A ceria-graphene oxide (ceria-GO) composite was fabricated by a hydrothermal reaction approach, resulting in the decoration of agglomerated ceria on the surface of graphene oxide (Sakthivel, Das, Pratt, & Seal, 2017). This composite showed a rapid adsorption of arsenic; the maximum adsorption capacities were 185 mg-As(III)/g and 212 mg-As(V)/g.

0.2-g/L ceria-GO composite was sufficient to meet the MCL for the simulated arsenic-contaminated water that had an initial concentration of

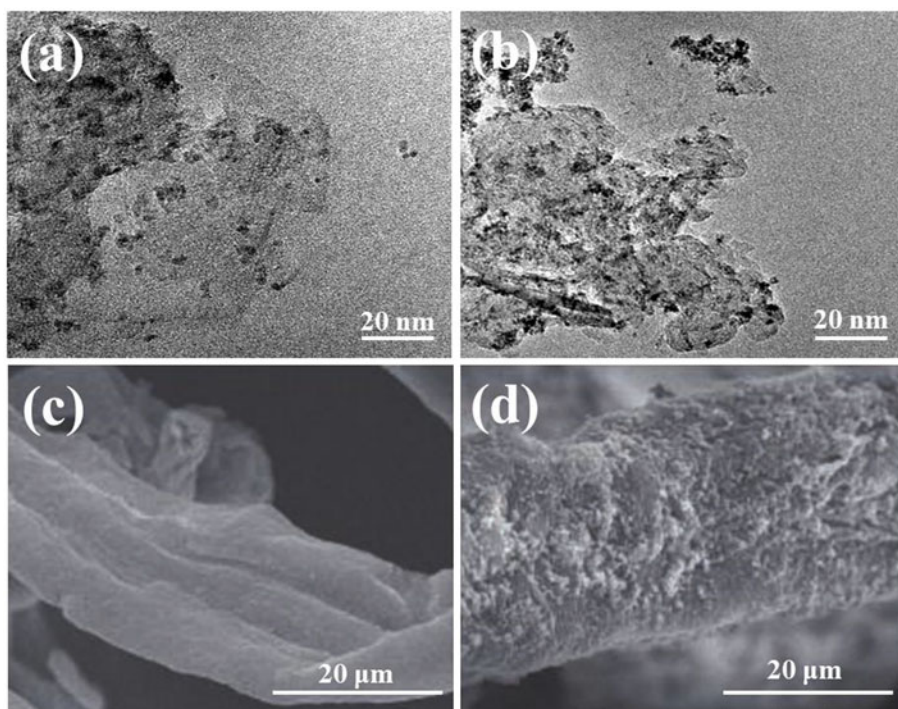


Figure 6. TEM images of the GNP-HCO adsorbent before (a) and after (b) As(V) adsorption (Yu et al., 2015) and FESEM images of the virgin cellulose fiber (c) and the cellulose fiber after coating Y(OH)₃ precipitate layer (d) (An et al., 2012).

0.1 mg-As/L. The arsenic was removed through binding onto the composite due to the electrostatic interaction and the formation of a stable complex compound with Ce(III). At low pH, the surfaces of ceria are positively charged, which enhances the removal of anionic As(V). Interestingly, the neutral As(III) removal was independent upon the surface charges of ceria. More work on the reusability and the competitive adsorption in the presence of the commonly existing anions is needed for the industrial-scale operation.

Biopolymers like chitosan are considered as attractive materials for the development of cost-effective adsorbents due to their abundant functional groups, impressive metal-binding capacity and environmental friendliness (Wu, Tseng, & Juang, 2001; Jayakumar, Nwe, Tokura, & Tamura, 2007; Yu, Deng & Yu, 2008; Zhu, Jiang, Xiao, & Li, 2010). An and coworkers (2012) developed a green adsorbent by coating the yttrium hydroxide precipitate layer on the cellulose fiber as shown in Figs. 6(c) and (d). The coating of yttrium hydroxide layer on cellulose fiber was established by the electrostatic interaction between the negatively charged cellulose fiber and the positively charged fresh precipitate (Wang, Wang, & Fang, 2005). Different from other studies (Chen, Zhu, Ma, Qiu, & Chen, 2013; Wilkie & Hering,

1996), the material exhibited favorable uptake capacity of both As(V) and As(III) at lower pH, while As(V) was favorably adsorbed with high selectivity against As(III) at pH 11.5.

A cerium modified cellulose ultrafine nanobioadsorbent (Ce-CNB) with the advantages of simultaneous oxidation and adsorption of As(III) was synthesized by precipitating the mixture of cellulose and Ce ions using 0.2-M NaOH followed by the further crosslinking by glutaraldehyde solution (Zhang, Zhu, Liu, & Zhang, 2016). The adsorption behavior was well described by the Langmuir isotherm and the pseudo-second-order kinetics equation; the maximum adsorption capacity of 57.5 mg-As/g for As(III) was found. Most of the competitive ions had little effects on the adsorption. Furthermore, the CE-CNB can be reused for multiple cycles; and 84% of the original As(III) adsorption capacity was retained after five cycles. The regeneration of this adsorbent was rather simple by using 0.1-M NaOH. The adsorption was due to a few mechanisms, being, (i) the formation of monodentate and bidentate complexes between hydroxyl groups and As(III), and (ii) partial oxidation of As(III) to As(V) followed by simultaneous adsorption on the adsorbent surface.

A bio-composite was prepared with ZnO, CeO₂, nanocellulose and polyaniline; it had a good removal efficiency for arsenic (Nath, Chaliha, Kalita, & Kalita, 2016). More importantly, it showed an obvious antibacterial property. The nanocellulose worked as a matrix for the integration of highly active ZnO and CeO₂ nanoparticles with the binding agent of polyaniline as shown in Fig. 7. The kinetics process was well fitted with the pseudo-second-order kinetics equation; this suggests that the adsorption might be mediated by the covalent chemisorption (Wahab, Jellali, & Jedidi, 2010). The adsorption isotherms of bio-composite were better described by the Freundlich and the Dubinin-Radushkevich equations than the Langmuir and the Temkin equations, indicating the occurrence of the adsorption of arsenic on the heterogeneous surface of the adsorbent. It was demonstrated that the adsorbent could be applied in the groundwater treatment that contained low concentrations of arsenic.

Volcanic rocks are readily available in several countries in the world such as Spain and Ethiopia. The adsorbents originated from these materials were tested for the removal of contaminants (Alemayehu & Lennartz, 2009). The Ce(IV) loaded volcanic rocks were used to treat As(III) and As(V)-contaminated water (Asere et al., 2017). The red scoria (Rs) and pumice (Pu) were loaded with cerium oxide. The pumice had a higher Ce(IV) loading due to its higher porosity than the Rs. The pseudo-second-order kinetics equation, and Freundlich and Dubinin-Radushkevich isotherms were used to model the adsorption data for both As(III) and As(V). The As(III) removal by both Ce-Rs and Ce-Pu was independent

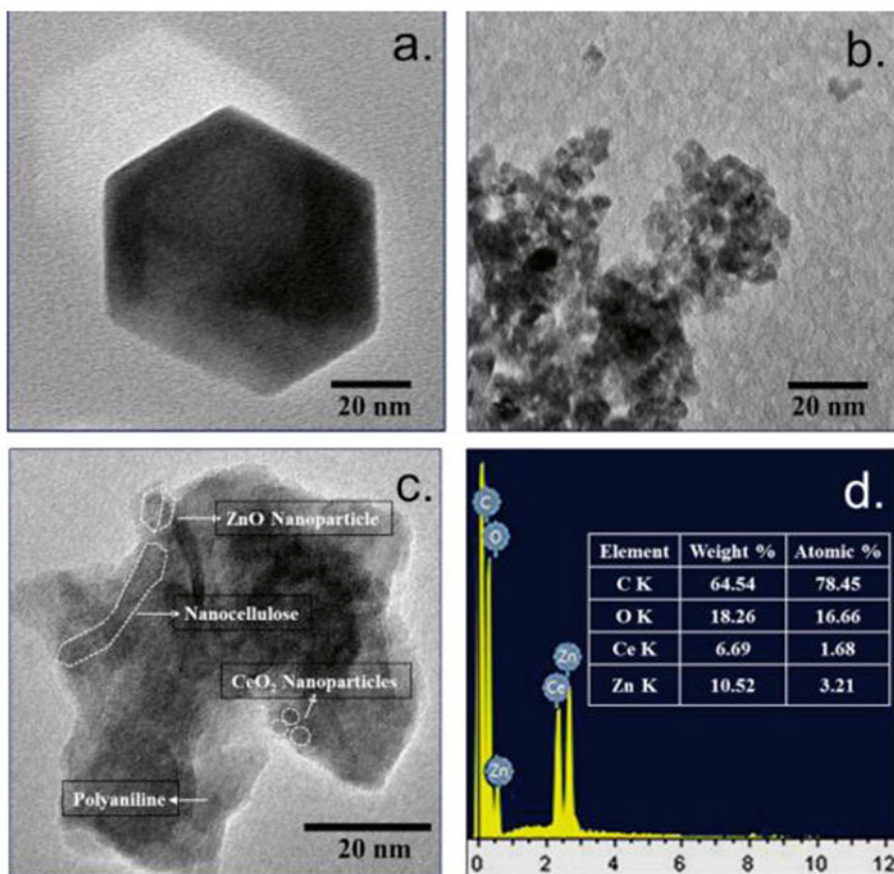


Figure 7. TEM images of ZnO nanoparticles (a), CeO₂ nanoparticles (b), and the ZnO:CeO₂:nanocellulose:polyaniline bio-composite (c); EDX element analysis of ZnO:CeO₂:nanocellulose:polyaniline bio-composite (d) (Nath et al., 2016).

upon the initial arsenic concentration. However, the As(V) removal increased with an increase in initial arsenic concentration. The maximum adsorption capacities of Ce-Rs and Ce-Pu were 0.643 mg-As(III)/g-Ce-Rs and 0.255 mg-As(V)/g-Ce-Rs, and 1.974 mg-As(III)/g-Ce-Pu and 0.893 mg-As(V)/g-Ce-Pu, respectively.

It was observed that phosphate ion as a competitive anion greatly influenced the adsorption of both Ce-loaded volcanic rocks while other anions did not retard the adsorption capacity greatly. In addition, the Ce-loaded volcanic rocks were able to retain high removal efficiency of As(III) and As(V) for several cycles; this indicates that they may be suitable for reuse and could be applied in the groundwater treatment where low-concentration phosphate exists.

A powdered activated carbon (PAC) was modified by an in-situ synthesis approach with the ceria particles, aiming to remove As(III) and As(V) ions (Sawana, Somasundar, Iyer, & Baruwati, 2017). The maximum uptake of

As(III) and As(V) by the PAC-CeO₂ occurred at pH 6 and 8, respectively. The experimental data was well fitted with the pseudo-second-order kinetics equation and the Freundlich isotherm. A removal of 80% was accomplished within 15 min. The adsorption performance of the modified PAC was greatly improved compared to the pristine PAC. The existence of phosphate ions in the arsenic-contaminated water caused a significant reduction of the arsenic removal. On the other hand, the presence of Cl⁻, SO₄²⁻ and humic acid had a slight impact on the adsorption. The spent adsorbent can be regenerated by using the natural hard water and reused for at least three cycles before the final arsenic concentration exceeded the MCL. The adsorption was due to an ion exchange between hydroxyl groups on ceria particles and arsenic from water.

A cerium oxide modified activated carbon was fabricated to treat high-concentration arsenic in water (Yu, Zhang, Yang, & Chen, 2017). The formation of cerium oxide partially blocked the pores of activated carbon, resulting in less specific surface area (414.4 m²/g) than the acid treated activated carbon (674.0 m²/g). The adsorbent achieved an optimal arsenic uptake at pH 5 with maximum adsorption capacities of 36.77 mg-As(III)/g and 43.60 mg-As(V)/g. The adsorption process was pH-dependent. The experimental data were well described by the Langmuir isotherm and the intraparticle pore diffusion model. In the presence of phosphate, the adsorption capacity of cerium oxide modified activated carbon was significantly reduced for both As(III) and As(V). On the contrary, the adsorption was slightly reduced by the existence of fluoride and humic acid.

The proposed mechanism for the arsenic removal was the ligand exchange between the hydroxyl groups on the surface of cerium oxide and arsenic species. Furthermore, the presence of Ce(IV) on the activated carbon caused the partial oxidation of As(III) to As(V) and facilitated the adsorption as As(V) is more readily adsorbed on the surface of adsorbent.

3.3. REM impregnated adsorbents

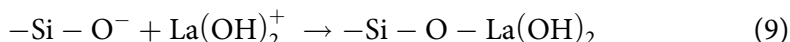
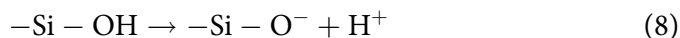
The above-mentioned support materials can also be used for loading REM ions through impregnation techniques so as to achieve high removal of arsenic. The metal ions can be well incorporated and uniformly distributed on the supporter surface via electrostatic interaction between them and the deprotonated functional groups (e.g., -OH and -COOH) on the inert supporters.

This section focuses on the adsorption mechanism of metal impregnated adsorbents and the influencing parameters, such as metal loading concentration, and pH. The performance of previously-reported metal ion impregnated adsorbents is listed in [Table 5](#).

Table 5. Rare-earth metal ion impregnated adsorbents used for arsenic removal.

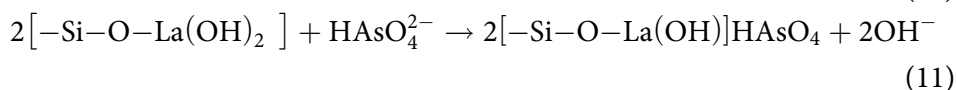
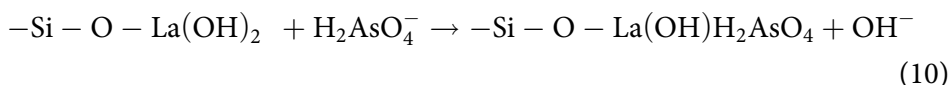
Metal ion	Supporter material	Loading amount of metal ion (mmol/g)	pH	Max. adsorption capacity (mg-As/g)		Ref.
				As(V)	As(III)	
La(III)	Amberlite 200CT resin	1.29	–	7.71	8.16	(Shao et al., 2008)
	Orange waste gel	0.55	6.5	42.0	43.0	(Biswas et al., 2008)
	Alumina	0.26	6-8	12.9	–	(Wasay et al., 1996)
	Zeolite X	1.10	5.0	30.75	–	(Haron et al., 2007)
	Zeolite ZSM 5	0.80	5.0	15.75	–	
	Zeolite A	0.58	5.0	14.25	–	
	Magnetized palm shell waste-based activated carbon	–	–	227.6	–	(Jais et al., 2016)
Ce(III)	Amberlite 200CT resin	1.29	–	53.57	34.44	(Shao et al., 2008)
	Orange waste gel	0.55	6.5	42.0	43.0	(Biswas et al., 2008)
	Amberlite IR-120 resin	1.55	6.0	2.384	2.5297	(He et al., 2012)
	Zeolite P	0.54	4.0	23.42	–	(Haron et al., 2008)
	Electrospun chitosan-polyvinyl alcohol nanofiber	0.11	6.2-7.0	–	18.0	(Sharma et al., 2014)
Ce(IV)	Fibrous protein	5.80	3-7	172.5	–	(Deng and Yu, 2012)
Y(III)	Amberlite resin	1.0	–	–	36.26	(Shao et al., 2008)
	Alumina	0.49	6-8	14.48	–	(Wasay et al., 1996)

The impregnation mechanism of REM ions onto supporter materials is given in the literatures (e.g., Wasay, Haran, & Tokunaga, 1996). For example, the lanthanum ions were successfully adsorbed onto silica gel through the following mechanisms:



According to Eq. (8), high pH would be favorable for the deprotonation of the hydroxyl groups on the silica gel. The similar results reported by Biswas et al. (2008) showed that the loading of La(III) and Ce(III) on gels became enhanced with an increase in solution pH and reached the maximum capacity at pH 5.5–6.5. At higher solution pH, the metal ions might precipitate as hydroxide, especially at concentrations of metal ions greater than 1 mM.

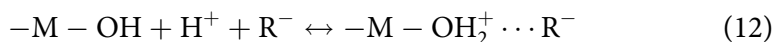
The mechanisms for the removal of arsenic by the chemical adsorption can be described as below (the equations are modified from those given by Wasay, Haran, & Tokunaga, 1996):



where $-\text{Si} - \text{O} - \text{La}(\text{OH})_2$ represents the lanthanum-impregnated silica gel, H_2AsO_4^- and HAsO_4^{2-} are predominant species of arsenic at neutral pH, and OH^- represents hydroxide ions released into solution.

Different from the mechanisms listed above (Wasay, Haran, & Tokunaga, 1996), the neutral water molecules may be also involved in the arsenic adsorption by the La(III)- and Ce(III)-loaded gels based on the fact that the solution pH may increase or keep constant after the adsorption. The exchangeable hydroxyl ions were formed during hydrolysis and participated in the adsorption process of arsenic via ligand exchange mechanism (Biswas et al., 2008).

The surface complexes between arsenic and REM impregnated adsorbents were also proposed to explain the adsorption mechanism (Deng & Yu, 2012). The hydroxyl groups on the Ce(IV)-impregnated fibrous protein could be protonated at low pH, leading to the positively charged surface on the adsorbent. The arsenic may be adsorbed due to chemical and electrostatic interactions between arsenic and the adsorbent according to the following scheme:



where M represents the metal ion Ce(IV), and R represents the arsenic anions.

As illustrated in Table 3, the selection of supporting materials greatly affects the performance of REM impregnated adsorbents for the arsenic removal. Three types of zeolites (Zeolite X, Zeolite ZSM 5, and Zeolite A) treated with lanthanum ions were employed for the As(V) adsorption from water (Haron, Masdan, Hussein, Zainal, & Kassim, 2007); it was shown that the loading amount of La ions and arsenic removal performance were dependent on the zeolite type. The content of functional groups on supporter materials was the key factor for the loading amount of metal(III) ions (Biswas et al., 2008). It was observed that the organic waste gels had the same loading capacity for the Ce(III) and La(III) ions (maximal uptake = 0.55 mol/kg). Meanwhile, similar maximum adsorption capacities of 43 mg-As/g for As(III) and 42 mg-As/g for As(V) were observed for both La(III)- and Ce(III)-loaded gels.

A different finding obtained by Shao et al. (2008) showed that the adsorption capacity of metal(III)-loaded amberlite 200CT resins toward As(III) followed by the order of: Y(III)-200CT > Ce(III)-200CT > Fe(III)-200CT > La(III)-200CT > Al(III)-200CT. This may result from the difference of operation conditions and initial concentrations of REMs.

Sharma et al. (2014) demonstrated that the adsorption of As(III) nearly linearly increased with an increase in the concentration of cerium ion (0.5 to 3.5%) in chitosan-polyvinyl alcohol (CHT/PVA) composite nanofibers. The viscosity of the solution increased when the concentration of Ce(III) in CHT/PVA was above 3.5%, leading to the non-uniform composite nanofibers and a decrease in the As(III) uptake. The temperature and solution pH may have some influences on the loading of metal ions.

3.4. Perspectives of REM based adsorbents in industrial applications

Various experimental evidences clearly show that the aforementioned REM based adsorbents have exceptional adsorption capacities for arsenic. These REM based adsorbents have relatively greater adsorption performance than the commercially available adsorbents and ion exchange resins. A few of them can have adsorption capacities as high as 480.2 mg-As/g (hydrated yttrium oxide, at pH 5) and 348.5 mg-As/g (Ti-loaded basic yttrium carbonate, at pH 7) (Lee et al., 2015; Yu et al., 2016). Furthermore, the adsorption can be completed within a short period of time. Therefore, the REM based adsorbents are especially suitable for treatment of highly arsenic-contaminated wastewater so as to reduce the arsenic to an acceptable level.

From the industrial standpoints, better operation for treatment of arsenic can be obtained by appropriately controlling several important parameters such as solution pH, dosage of adsorbent, and contact time. pH monitoring and adjustment are of great importance in the performance of REM based adsorbents in the water treatment.

Furthermore, the cost and complexity of large-scale synthesis and industrial applications of the adsorbents are largely affected by their physical and chemical properties. The REM based metal oxides/hydroxides can be more facially and economically synthesized by the coprecipitation approaches than the hydrothermal or solvothermal ones. The REM impregnated adsorbents and the REM oxide/hydroxide modified adsorbents can be developed by filtering the REM-containing solution through the supporters in a packed column, followed by the circulating filtration of the basic solution (e.g., NaOH).

A packed column containing REM oxide/hydroxide modified adsorbents or the REM ion impregnated adsorbents can then be applied for the arsenic decontamination. After most of adsorption capacity is reached (e.g., 75% of saturation determined by lab-scale studies), the spent adsorbent in the packed column can be recovered by the regenerating solution.

On contrary, the application of REM oxides/hydroxides for arsenic decontamination is mainly limited by the challenge in the collection/separation of the spent adsorbents from the treated water. Centrifugation or filtration is generally required for the separation, which is both energy-consuming and costly. The adsorption performance of REM oxide/hydroxide modified or REM ion impregnated adsorbents is highly dependent on the loading amount of REM oxides/hydroxides or ions.

For the REM impregnated adsorbents, the REM ions are fixed on the supporter surface via chemical and electrostatic interactions between them and deprotonated functional groups on the supporter. The leaching problem of REM ions, especially under strongly acidic conditions, may lead to

an obvious reduction of adsorption capacity of the adsorbents. Thus, better control in the solution would be essential for the industrial operations.

There are certain drawbacks of these adsorbents when we compare them with commercially available adsorbents. The key information of important adsorbents, namely adsorption capacity, reusability and roughly estimated cost is shown in Table 6.

The cost of REM based adsorbents is relatively higher than that of commercially available adsorbents. In addition, the regeneration and reuse of spent adsorbents have yet to reach the industrial satisfaction level. More research work should be done so as to find out the optimal procedures in the regeneration and reuse.

Generally speaking, the adsorptive performance of the adsorbents is retarded under alkaline conditions. The arsenic uptake is mainly dominated by the ion exchange process and complex formation, followed by the electrostatic interaction. Alkaline solution, e.g., 0.1-M NaOH, is therefore more suitable for the regeneration of the spent adsorbents than acid or salt solutions (Feng et al., 2012; Zhang, He, & Xu, 2012). For instance, the regeneration efficiency of As(V)-loaded CeO₂-CNT can reach above 94% when 0.1-M NaOH was used (Peng et al., 2005).

The adsorption performance of adsorbents for the arsenic removal easily becomes deteriorated in the presence of competitive phosphate and fluoride ions. However, such a problem is less obvious for treatment of arsenic in surface and groundwater as the concentrations of phosphate and/or fluoride are low. On the other hand, the adsorbents can effectively remove both phosphate and fluoride ions in the aqueous solutions, which are documented in the literatures (e.g., Yu & Chen, 2014).

To compensate the drawbacks, the REM based adsorbents were modified with commonly existing metals (e.g., Al, Mg, and Fe) or loaded on organic supporters. The modification of the adsorbents can reduce the interference of competitive anions and maintain high adsorption capacity for arsenic removal.

In addition, the cost of adsorbents can be diminished by using the REM as the additive in the production of conventional adsorbents (e.g., based on

Table 6. Comparison of rare-earth metal and conventional metal based adsorbents.

Adsorbent	Adsorption capacity (mg-As/g)	Reusability	Estimated cost level	Ref.
Basic aluminium carbonate	170 (As(V))	–	Low	(Shao et al., 2008)
Ti-loaded basic yttrium carbonate	348.5 (As(V))	Only two cycles	Moderate	(Lee et al., 2015)
Chestnut-like Fe ₂ O ₃	137.5 (As(V))	–	Low	(Wasay et al., 1996)
Hydrous cerium oxide	107.1 (As(V))	–	High	(Li et al., 2012)
	171.88 (As(III))			
Hollow nestlike α -Fe ₂ O ₃	75.3 (As(V))	Reusable	Low	(Haron et al., 2007)
Mesoporous Ce-Fe oxide	91.74 (As(V))	At least five cycles	Moderate	(Chen et al., 2013)
Fe-Mn binary oxide	63.8 (As(V)),	–	Low	(Zhang et al., 2007)
	73.5 (As(III))			

commonly existing metals). The resulted adsorbents can outperform the pure REM based adsorbents. However, the regeneration and reuse studies on these modified adsorbents are needed since regenerative capability of the adsorbents is one of the major concerns for the industrial applications. Therefore, extensive future studies on the modification of pure REM based adsorbents and reusability of the adsorbents are important to offset the drawbacks of pure REM based adsorbents and provide great opportunities of these adsorbents in the removal of arsenic from industrial wastewater or groundwater.

4. Conclusions

The unique physio-chemical properties of REMs and their excellent removal efficiency toward arsenic have attracted growing attentions in academic and industrial communities. In this review article, the characteristics of the REMs and the adsorption performance of the REM based adsorbents previously reported were systemically reviewed and commented. These adsorbents were compared with a group of commonly reported adsorbents for the adsorption performances. The multiple-species REM based adsorbents outperform the single-species REM based adsorbents due to their lower cost, higher arsenic uptake, and better stability. The functional groups on the adsorbent surface (e.g., -OH and CO_3^{2-}) can greatly be involved in the adsorption process via the ligand exchange, the complex formation, and the electrostatic interaction. The adsorption rate can be further improved by loading the REM oxides/hydroxides or REM ions onto the porous materials of higher surface area and larger porosity. Although the adsorption capacity of REM based adsorbents is greater than the commonly existing metal based adsorbents (e.g., iron oxide), the reusability of REM based adsorbents is uncertain. In consideration of the great application potential of REM based adsorbents for the water treatment, there is still a room for further R&D so that they can be used by the industries successfully.

Acknowledgments

YY and KYK thank National University of Singapore providing President's Graduate Fellowship for their PhD study. LY and CHW would like to give appreciation to NUS for the 4-year PhD scholarship.

Funding

This research project is partially supported by the National Research Foundation, Prime Minister's Office, Singapore under its Campus for Research Excellence and Technological Enterprise (CREATE) program.

ORCID

J. Paul Chen  <http://orcid.org/0000-0002-9964-293X>

References

- Alemayehu, E., & Lennartz, B. (2009). Virgin volcanic rocks: Kinetics and equilibrium studies for the adsorption of cadmium from water. *Journal of Hazardous Materials*, 169(1–3), 395–401.
- An, M. I., Zhang, X., Yang, T., Chen, M., & Wang, J. (2012). Uptake and speciation of inorganic arsenic with cellulose fibre coated with yttrium hydroxide layer as a novel green sorbent. *Chinese Journal of Chemistry*, 30(9), 2225–2231.
- Anawar, H., Akai, J., Mostofa, K., Safiullah, S., & Tareq, S. (2002). Arsenic poisoning in groundwater: Health risk and geochemical sources in Bangladesh. *Environment International*, 27(7), 597–604.
- Anderson, M. A., Ferguson, J. F., & Gavis, J. (1976). Arsenate adsorption on amorphous aluminum hydroxide. *Journal of Colloid and Interface Science*, 54(3), 391–399.
- Asere, T. G., Verbeken, K., Tessema, D. A., Fufa, F., Stevens, C. V., & Du, L. G. (2017). Adsorption of As(III) versus As(V) from aqueous solutions by cerium-loaded volcanic rocks. *Environmental Science and Pollution Research International*, 24(25), 20446–20458.
- Babaeiveli, K., Khodadoust, A. P., & Bogdan, D. (2014). Adsorption and removal of arsenic (V) using crystalline manganese (II,III) oxide: Kinetics, equilibrium, effect of pH and ionic strength. *Journal of Environmental Science & Health Part A*, 49(13), 1462–1473.
- Bailey, S. E., Olin, T. J., Bricka, R. M., & Adrian, D. D. (1999). A review of potentially low-cost sorbents for heavy metals. *Water Research*, 33(11), 2469–2479.
- Barkam, S., Ortiz, J., Saraf, S., Eliason, N., McCormack, R., Das, S., ... Hanson, C. (2017). Modulating the catalytic activity of cerium oxide nanoparticles with the anion of the precursor salt. *The Journal of Physical Chemistry C*, 121(36), 20039.
- Basu, T., & Ghosh, U. C. (2013). Nano-structured iron(III)–cerium(IV) mixed oxide: Synthesis, characterization and arsenic sorption kinetics in the presence of co-existing ions aiming to apply for high arsenic groundwater treatment. *Applied Surface Science*, 283, 471–481.
- Bhattacharya, S., Gupta, K., & Ghosh, U. C. (2017). Synthesis, characterization and trivalent arsenic sorption potential of Ce-Al nanostructured mixed oxide. *IOP Conference Series: Materials Science and Engineering*, 188, 012003.
- Bhattacharyya, K. G., & Gupta, S. S. (2008). Adsorption of a few heavy metals on natural and modified kaolinite and montmorillonite: A review. *Advances in Colloid and Interface Science*, 140(2), 114–131.
- Biswas, B. K., Inoue, K., Ghimire, K. N., Kawakita, H., Ohto, K., & Harada, H. (2008). Effective removal of arsenic with lanthanum(III)- and cerium(III)-loaded orange waste gels. *Separation Science & Technology*, 43(8), 2144–2165.
- Breck, D. W. (1974). *Zeolite molecular sieves: Structure, chemistry, and use*. New York: Wiley.
- Chen, C.-C., Do, J.-S., & Gu, Y. (2009). Immobilization of HRP in mesoporous silica and its application for the construction of polyaniline modified hydrogen peroxide biosensor. *Sensors*, 9(6), 4635–4648.
- Cheng, W., Zhang, W., Hu, L., Ding, W., Wu, F., & Li, J. (2016). Etching synthesis of iron oxide nanoparticles for adsorption of arsenic from water. *RSC Advances*, 6(19), 15900–15910.

- Chen, G., Xu, C., Song, X., Xu, S., Ding, Y., & Sun, S. (2008). Template-free synthesis of single-crystalline-like CeO₂ hollow nanocubes. *Crystal Growth and Design*, 8(12), 4449–4453.
- Chen, B., Zhu, Z., Guo, Y., Qiu, Y., & Zhao, J. (2013). Facile synthesis of mesoporous Ce–Fe bimetal oxide and its enhanced adsorption of arsenate from aqueous solutions. *Journal of Colloid and Interface Science*, 398, 142–151.
- Chen, B., Zhu, Z., Liu, S., Hong, J., Ma, J., Qiu, Y., & Chen, J. (2014a). Facile hydrothermal synthesis of nanostructured hollow iron–cerium alkoxides and their superior arsenic adsorption performance. *ACS Applied Materials & Interfaces*, 6(16), 14016–14025.
- Chen, B., Zhu, Z., Hong, J., Wen, Z., Ma, J., Qiu, Y., & Chen, J. (2014b). Nanocasted synthesis of ordered mesoporous cerium iron mixed oxide and its excellent performances for As(V) and Cr(VI) removal from aqueous solutions. *Dalton Transactions*, 43(28), 10767–10777.
- Chen, B., Zhu, Z., Ma, J., Qiu, Y., & Chen, J. (2013). Surfactant assisted Ce–Fe mixed oxide decorated multiwalled carbon nanotubes and their arsenic adsorption performance. *Journal of Materials Chemistry A*, 1(37), 11355–11367.
- Chong, S., Holmstrom, D., Li, Q., & Tong, O. (2009). Preparation and evaluation of a Ce (IV)–La (III) binary hydroxide adsorbent as recovery of waste ceria powder from glass polishing process for effective arsenic removal. *Vatten*, 65, 193–200.
- Cotton, S. (2013). *Lanthanide and actinide chemistry*. Chichester, UK: John Wiley & Sons.
- Cotton, S. A. (1994). *Scandium, Yttrium & the Lanthanides: Inorganic & Coordination Chemistry. Encyclopedia of inorganic chemistry*, Chichester, UK: John Wiley & Sons.
- Deng, S., Li, Z., Huang, J., & Yu, G. (2010). Preparation, characterization and application of a Ce–Ti oxide adsorbent for enhanced removal of arsenate from water. *Journal of Hazardous Materials*, 179(1–3), 1014–1021.
- Deng, H., & Yu, X. (2012). Adsorption of fluoride, arsenate and phosphate in aqueous solution by cerium impregnated fibrous protein. *Chemical Engineering Journal*, 184, 205–212.
- Fang, Y. P., Xu, A. W., You, L. P., Song, R. Q., Yu, J. C., Zhang, H. X., ... Liu, H. Q. (2003). Hydrothermal synthesis of Rare Earth (TB, Y) hydroxide and oxide nanotubes. *Advanced Functional Materials*, 13, 955–960.
- Feng, Q., Zhang, Z., Ma, Y., He, X., Zhao, Y., & Chai, Z. (2012). Adsorption and desorption characteristics of arsenic onto ceria nanoparticles. *Nanoscale Research Letters*, 7(1), 84.
- Giles, D. E., Mohapatra, M., Issa, T. B., Anand, S., & Singh, P. (2011). Iron and aluminium based adsorption strategies for removing arsenic from water. *Journal of Environmental Management*, 92(12), 3011–3022.
- Gojny, F. H., Wichmann, M. H., Fiedler, B., Bauhofer, W., & Schulte, K. (2005). Influence of nano-modification on the mechanical and electrical properties of conventional fibre-reinforced composites. *Composites Part A: Applied Science and Manufacturing*, 36(11), 1525–1535.
- Gregg, S. J., Sing, K. S. W., & Salzberg, H. (1967). Adsorption surface area and porosity. *Journal of the Electrochemical Society*, 114(11), 279C.
- Gschneider, K. A. (1966). *Rare earths: the fraternal fifteen*, Oak Ridge. Tennessee, US: United States Atomic Energy Commission, Division of Technical Information.
- Guo, Y., Zhu, Z., Qiu, Y., & Zhao, J. (2012). Adsorption of arsenate on Cu/Mg/Fe/La layered double hydroxide from aqueous solutions. *Journal of Hazardous Materials*, 239–240, 279–288.
- Gupta, K., Bhattacharya, S., Chattopadhyay, D., Mukhopadhyay, A., Biswas, H., Dutta, J., ... Ghosh, U. C. (2011). Ceria associated manganese oxide nanoparticles: Synthesis,

- characterization and arsenic(V) sorption behavior. *Chemical Engineering Journal*, 172(1), 219–229.
- Gupta, A., Das, S., Neal, C. J., & Seal, S. (2016). Controlling the surface chemistry of cerium oxide nanoparticles for biological applications. *Journal of Materials Chemistry B*, 4(19), 3195–3202.
- Hall, A. H. (2002). Chronic arsenic poisoning. *Toxicology Letters*, 128(1–3), 69–72.
- Haron, M. J., Ab Rahim, F., Abdullah, A. H., Hussein, M. Z., & Kassim, A. (2008). Sorption removal of arsenic by cerium-exchanged zeolite P. *Materials Science and Engineering: B*, 149(2), 204–208.
- Haron, M. J., Masdan, S. A., Hussein, M. Z., Zainal, Z., & Kassim, A. (2007). Kinetics and thermodynamic for sorption of arsenate by lanthanum-exchanged zeolite. *The Malaysian Journal of Analytical Sciences*, 15, 219–228.
- He, Z., Tian, S., & Ning, P. (2012). Adsorption of arsenate and arsenite from aqueous solutions by cerium-loaded cation exchange resin. *Journal of Rare Earths*, 30(6), 563–572.
- Hirano, M., & Kato, E. (1996). The hydrothermal synthesis of ultrafine cerium(IV) oxide powders. *Journal of Materials Science Letters*, 15(14), 1249–1250.
- Hui, B., Zhang, Y., & Ye, L. (2015). Structure of PVA/gelatin hydrogel beads and adsorption mechanism for advanced Pb (II) removal. *Journal of Industrial and Engineering Chemistry*, 21, 868–876.
- Inoue, M., Kimura, M., & Inui, T. (1999). Transparent colloidal solution of 2 nm ceria particles. *Chemical Communications*, 11(11), 957–958.
- Jais, F. M., Ibrahim, S., Yoon, Y., & Jang, M. (2016). Enhanced arsenate removal by lanthanum and nano-magnetite composite incorporated palm shell waste-based activated carbon. *Separation and Purification Technology*, 169, 93–102.
- Jang, M., Park, J. K., & Shin, E. W. (2004). Lanthanum functionalized highly ordered mesoporous media: Implications of arsenate removal. *Microporous and Mesoporous Materials*, 75(1–2), 159–168.
- Jayakumar, R., Nwe, N., Tokura, S., & Tamura, H. (2007). Sulfated chitin and chitosan as novel biomaterials. *International Journal of Biological Macromolecules*, 40(3), 175–181.
- Jennifer, L. M. R., Drobek, T., Rossi, A., & Gauckler, L. J. (2007). Chemical analysis of spray pyrolysis gadolinia-doped ceria electrolyte thin films for solid oxide fuel cells. *Chemistry of Materials*, 19(5), 1134–1142.
- Jiao, F., Harrison, A., Jumas, J.-C., Chadwick, A. V., Kockelmann, W., & Bruce, P. G. (2006). Ordered mesoporous Fe₂O₃ with crystalline walls. *Journal of the American Chemical Society*, 128(16), 5468–5474.
- Jomekian, A., Pakizeh, M., Shafiee, A. R., & Mansoori, S. A. A. (2011). Fabrication or preparation and characterization of new modified MCM-41/PSf nanocomposite membrane coated by PDMS. *Separation and Purification Technology*, 80(3), 556–565.
- Kapaj, S., Peterson, H., Liber, K., & Bhattacharya, P. (2006). Human health effects from chronic arsenic poisoning—a review. *Journal of Environmental Science and Health Part A*, 41(10), 2399–2428.
- Kesraoui-Ouki, S., Cheeseman, C. R., & Perry, R. (1994). Natural zeolite utilisation in pollution control: A review of applications to metals' effluents. *Journal of Chemical Technology and Biotechnology*, 59(2), 121–126.
- Kim, J., & Benjamin, M. M. (2004). Modeling a novel ion exchange process for arsenic and nitrate removal. *Water Research*, 38(8), 2053–2062.
- Krishna, B., Murty, D., & Prakash, B. J. (2000). Thermodynamics of chromium (VI) anionic species sorption onto surfactant-modified montmorillonite clay. *Journal of Colloid and Interface Science*, 229(1), 230–236.

- Lee, H., & Choi, W. (2002). Photocatalytic oxidation of arsenite in TiO₂ suspension: Kinetics and mechanisms. *Environmental Science & Technology*, 36(17), 3872–3878.
- Lee, S.-H., Kim, K.-W., Lee, B.-T., Bang, S., Kim, H., Kang, H., & Jang, A. (2015). Enhanced arsenate removal performance in aqueous solution by yttrium-based adsorbents. *International Journal of Environmental Research and Public Health*, 12(10), 13523–13541.
- Li, Z., Deng, S., Yu, G., Huang, J., & Lim, V. C. (2010). As(V) and As(III) removal from water by a Ce–Ti oxide adsorbent: Behavior and mechanism. *Chemical Engineering Journal*, 161(1–2), 106–113.
- Li, Y., Ding, J., Chen, J., Xu, C., Wei, B., Liang, J., & Wu, D. (2002). Preparation of ceria nanoparticles supported on carbon nanotubes. *Materials Research Bulletin*, 37(2), 313–318.
- Li, R., Li, Q., Gao, S., & Shang, J. K. (2012). Exceptional arsenic adsorption performance of hydrous cerium oxide nanoparticles: Part A. Adsorption capacity and mechanism. *Chemical Engineering Journal*, 185–186, 127–135.
- Lin, S.-H., & Juang, R.-S. (2002). Heavy metal removal from water by sorption using surfactant-modified montmorillonite. *Journal of Hazardous Materials*, 92(3), 315–326.
- Lin, S.-H., & Juang, R.-S. (2009). Adsorption of phenol and its derivatives from water using synthetic resins and low-cost natural adsorbents: A review. *Journal of Environmental Management*, 90(3), 1336–1349.
- Mazumder, D. N. G., Haque, R., Ghosh, N., De Binay, K., Santra, A., Chakraborty, D., & Smith, A. H. (1998). Arsenic levels in drinking water and the prevalence of skin lesions in West Bengal, India. *International Journal of Epidemiology*, 27(5), 871–877.
- Miao, Q., Xiong, G., Sheng, S., Cui, W., Xu, L., & Guo, X. (1997). Partial oxidation of methane to syngas over nickel-based catalysts modified by alkali metal oxide and rare earth metal oxide. *Applied Catalysis A: General*, 154(1–2), 17–27.
- Moeller, T., & Ferrus, R. (1961). Observations on the rare earths—LXXIII the heat and entropy of formation of the 1: 1 chelates of N-hydroxyethylethylenediaminetriacetic acid with the tripositive cations. *Journal of Inorganic and Nuclear Chemistry*, 20(3–4), 261–273.
- Nath, B. K., Chaliha, C., Kalita, E., & Kalita, M. C. (2016). Synthesis and characterization of ZnO:CeO₂: nanocellulose:PANI bionanocomposite. A bimodal agent for arsenic adsorption and antibacterial action. *Carbohydrate Polymers*, 148, 397–405.
- Ou, E., Zhou, J., Mao, S., Wang, J., Xia, F., & Min, L. (2007). Highly efficient removal of phosphate by lanthanum-doped mesoporous SiO₂. *Colloids and Surfaces A: Physicochemical and Engineering Aspects*, 308(1–3), 47–53.
- Paulenova, A., Creager, S. E., Navratil, J., & Wei, Y. (2002). Redox potentials and kinetics of the Ce³⁺/Ce⁴⁺ redox reaction and solubility of cerium sulfates in sulfuric acid solutions. *Journal of Power Sources*, 109(2), 431–438.
- Pearson, R. G. (1990). Hard and soft acids and bases—the evolution of a chemical concept. *Coordination Chemistry Reviews*, 100, 403–425.
- Peng, X., Luan, Z., Ding, J., Di, Z., Li, Y., & Tian, B. (2005). Ceria nanoparticles supported on carbon nanotubes for the removal of arsenate from water. *Materials Letters*, 59(4), 399–403.
- Planeix, J., Coustel, N., Coq, B., Brotons, V., Kumbhar, P., Dutartre, R., ... Ajayan, P. (1994). Application of carbon nanotubes as supports in heterogeneous catalysis. *Journal of the American Chemical Society*, 116(17), 7935–7936.
- Pu, H., Huang, J. & Jiang, Z. (2008). *Removal of Arsenic (V) from Aqueous Solutions by Lanthanum - loaded Zeolite*. *Acta Geologica Sinica (English Edition)* 82, 1015–1019.

- Pramanik, M., Srivastava, S., Samantaray, B., & Bhowmick, A. (2001). Preparation and properties of ethylene vinyl acetate-clay hybrids. *Journal of Materials Science Letters*, 20(15), 1377–1380.
- Rahman, M. A., Rahman, M. A., Samad, A., & Alam, A. M. (2008). Removal of arsenic with oyster shell: Experimental measurements. *Pakistan Journal of Analytical & Environmental Chemistry*, 9, 69–77.
- Raichur, A., & Panvekar, V. (2002). Removal of As (V) by adsorption onto mixed rare earth oxides. *Separation Science and Technology*, 37(5), 1095–1108.
- Ravenscroft, P., Brammer, H., & Richards, K. (2009). *Arsenic pollution: A global synthesis*. Malden, Mass, US: John Wiley & Sons.
- Sabbatini, P., Yrazu, F., Rossi, F., Thern, G., Marajofsky, A., & Fidalgo de Cortalezzi, M. M. (2010). Fabrication and characterization of iron oxide ceramic membranes for arsenic removal. *Water Research*, 44(19), 5702–5712.
- Sahu, U. K., Sahu, M. K., Mohapatra, S. S., & Patel, R. K. (2016). Removal of As (V) from aqueous solution by Ce-Fe bimetal mixed oxide. *Journal of Environmental Chemical Engineering*, 4(3), 2892–2899.
- Sakthivel, T., Das, S., Kumar, A., Reid, D. L., Gupta, A., Sayle, D. C., & Seal, S. (2013). Morphological phase diagram of biocatalytically active ceria nanostructures as a function of processing variables and their properties. *Chempluschem*, 78(12), 1446–1455.
- Sakthivel, T. S., Das, S., Pratt, C. J., & Seal, S. (2017). One-pot synthesis of a ceria-graphene oxide composite for the efficient removal of arsenic species. *Nanoscale*, 9(10), 3367–3374.
- Sawana, R., Somasundar, Y., Iyer, V. S., & Baruwati, B. (2017). Ceria modified activated carbon: An efficient arsenic removal adsorbent for drinking water purification. *Applied Water Science*, 7(3), 1223–1230.
- Seida, Y., & Izumi, Y. (2005). Synthesis of clay–cerium hydroxide conjugates for the adsorption of arsenic. *Adsorption Science & Technology*, 23(8), 607–618.
- Sen, I. S., & Peucker-Ehrenbrink, B. (2012). Anthropogenic disturbance of element cycles at the earth's surface. *Environmental Science & Technology*, 46(16), 8601–8609.
- Shao, W., Li, X., Cao, Q., Luo, F., Li, J., & Du, Y. (2008). Adsorption of arsenate and arsenite anions from aqueous medium by using metal(III)-loaded amberlite resins. *Hydrometallurgy*, 91(1–4), 138–143.
- Sharma, R., Singh, N., Gupta, A., Tiwari, S., Tiwari, S. K., & Dhakate, S. R. (2014). Electrospun chitosan-polyvinyl alcohol composite nanofibers loaded with cerium for efficient removal of arsenic from contaminated water. *Journal of Materials Chemistry A*, 2(39), 16669–16677.
- Shukla, D. P., Dubey, C. S., Singh, N. P., Tajbakhsh, M., & Chaudhry, M. (2010). Sources and controls of Arsenic contamination in groundwater of Rajnandgaon and Kanker District, Chattisgarh Central India. *Journal of Hydrology*, 395(1–2), 49–66.
- Srivastava, P. K., Vaish, A., Dwivedi, S., Chakrabarty, D., Singh, N., & Tripathi, R. D. (2011). Biological removal of arsenic pollution by soil fungi. *The Science of the Total Environment*, 409(12), 2430–2442.
- Sun, W., Li, Q., Gao, S., & Shang, J. K. (2012). Exceptional arsenic adsorption performance of hydrous cerium oxide nanoparticles: Part B. Integration with silica monoliths and dynamic treatment. *Chemical Engineering Journal*, 185–186, 136–143.
- Sun, C., Li, H., Zhang, H., Wang, Z., & Chen, L. (2005). Controlled synthesis of CeO₂ nanorods by a solvothermal method. *Nanotechnology*, 16(9), 1454.
- Taniguchi, T., Watanabe, T., Sakamoto, N., Matsushita, N., & Yoshimura, M. (2008). Aqueous route to size-controlled and doped organophilic ceria nanocrystals. *Crystal Growth and Design*, 8(10), 3725–3730.

- Tokunaga, S., Wasay, S. A., & Park, S.-W. (1997). Removal of arsenic (V) ion from aqueous solutions by lanthanum compounds. *Water Science and Technology*, 35(7), 71–78.
- Vinu, A., Murugesan, V., & Hartmann, M. (2004). Adsorption of lysozyme over mesoporous molecular sieves MCM-41 and SBA-15: Influence of pH and aluminum incorporation. *The Journal of Physical Chemistry B*, 108(22), 7323–7330.
- Wahab, M. A., Jellali, S., & Jedidi, N. (2010). Ammonium biosorption onto sawdust: FTIR analysis, kinetics and adsorption isotherms modeling. *Bioresource Technology*, 101(14), 5070–5075.
- Wang, H.-J., Gong, W.-X., Liu, R.-P., Liu, H.-J., & Qu, J.-H. (2011). Treatment of high arsenic content wastewater by a combined physical–chemical process. *Colloids and Surfaces A: Physicochemical and Engineering Aspects*, 379(1–3), 116–120.
- Wang, Y.-J., Ji, F., Wang, W., Yuan, S.-J., & Hu, Z.-H. (2015). Removal of roxarsone from aqueous solution by Fe/La-modified montmorillonite. *Desalination and Water Treatment*, 57(43), 1–14.
- Wang, C., Lee, M., Liu, X., Wang, B., Chen, J. P., & Li, K. (2016). Metal-organic framework/ α -alumina composite with novel geometry for enhanced adsorptive separation. *Chemical Communications*, 52(57), 8869.
- Wang, C., Liu, X., Chen, J. P., & Li, K. (2015). Superior removal of arsenic from water with zirconium metal-organic framework UiO-66. *Scientific Reports*, 5(1), 16613.
- Wang, S., & Mulligan, C. N. (2006). Occurrence of arsenic contamination in Canada: Sources, behavior and distribution. *The Science of the Total Environment*, 366(2–3), 701–721.
- Wang, Y., Wang, J.-H., & Fang, Z.-L. (2005). Octadecyl immobilized surface for precipitate collection with a renewable microcolumn in a lab-on-valve coupled to an electrothermal atomic absorption spectrometer for ultratrace cadmium determination. *Analytical Chemistry*, 77(16), 5396–5401.
- Wasay, S., Haran, M. J., & Tokunaga, S. (1996). Adsorption of fluoride, phosphate, and arsenate ions on lanthanum-impregnated silica gel. *Water Environment Research*, 68(3), 295–300.
- Wasay, S. A., Tokunaga, S., & Park, S.-W. (1996). Removal of hazardous anions from aqueous solutions by La (III)-and Y (III)-impregnated alumina. *Separation Science and Technology*, 31(10), 1501–1514.
- Wei, Y.-T., Zheng, Y.-M., & Paul Chen, J. (2011). Enhanced adsorption of arsenate onto a natural polymer-based sorbent by surface atom transfer radical polymerization. *Journal of Colloid and Interface Science*, 356(1), 234–239.
- Wilkie, J. A., & Hering, J. G. (1996). Adsorption of arsenic onto hydrous ferric oxide: Effects of adsorbate/adsorbent ratios and co-occurring solutes. *Colloids and Surfaces A: Physicochemical and Engineering Aspects*, 107, 97–110.
- Wu, S.-H., Mou, C.-Y., & Lin, H.-P. (2013). Synthesis of mesoporous silica nanoparticles. *Chemical Society Reviews*, 42(9), 3862–3875.
- Wu, F.-C., Tseng, R.-L., & Juang, R.-S. (2001). Kinetic modeling of liquid-phase adsorption of reactive dyes and metal ions on chitosan. *Water Research*, 35(3), 613–618.
- Wu, Z.-S., Zhou, G., Yin, L.-C., Ren, W., Li, F., & Cheng, H.-M. (2012). Graphene/metal oxide composite electrode materials for energy storage. *Nano Energy*, 1(1), 107–131.
- Xiao, H., Ai, Z., & Zhang, L. (2009). Nonaqueous sol-gel synthesized hierarchical CeO₂ nanocrystal microspheres as novel adsorbents for wastewater treatment. *The Journal of Physical Chemistry C*, 113(38), 16625–16630.
- Xu, P., Yang, J., Wang, K., Zhou, Z., & Shen, P. (2012). Porous graphene: Properties, preparation, and potential applications. *Chinese Science Bulletin*, 57(23), 2948–2955.

- Yan, L., Tu, H., Chan, T., & Jing, C. (2017). Mechanistic study of simultaneous arsenic and fluoride removal using granular TiO₂-La adsorbent. *Chemical Engineering Journal*, 313, 983.
- Yin, H., Zhao, S., Wan, J., Tang, H., Chang, L., He, L., ... Tang, Z. (2013). Three-dimensional graphene/metal oxide nanoparticle hybrids for high-performance capacitive deionization of saline water. *Advanced Materials*, 25(43), 6270–6276.
- Yu, Y., & Chen, J. P. (2014). Fabrication and performance of a Mn-La metal composite for remarkable decontamination of fluoride. *Journal of Materials Chemistry A*, 2(21), 8086–8093.
- Yu, Q., Deng, S., & Yu, G. (2008). Selective removal of perfluorooctane sulfonate from aqueous solution using chitosan-based molecularly imprinted polymer adsorbents. *Water Research*, 42(12), 3089–3097.
- Yu, L., Ma, Y., Ong, C. N., Xie, J., & Liu, Y. (2015). Rapid adsorption removal of arsenate by hydrous cerium oxide-graphene composite. *RSC Advances*, 5(80), 64983–64990.
- Yu, Y., Yu, L., & Chen, J. P. (2015). Introduction of an yttrium-manganese binary composite that has extremely high adsorption capacity for arsenate uptake in different water conditions. *Industrial & Engineering Chemistry Research*, 54(11), 3000–3008.
- Yu, Y., Yu, L., Sun, M., & Chen, J. P. (2016). Facile synthesis of highly active hydrated yttrium oxide towards arsenate adsorption. *Journal of Colloid and Interface Science*, 474, 216–222.
- Yu, Y., Zhang, C., Yang, L., & Chen, J. P. (2017). Cerium oxide modified activated carbon as an efficient and effective adsorbent for the rapid uptake of arsenate and arsenite: Material development and study of performance and mechanisms. *Chemical Engineering Journal*, 315, 630–638.
- Yu, Y., Zhao, C., Wang, Y., Fan, W., & Luan, Z. (2013). Effects of ion concentration and natural organic matter on arsenic(V) removal by nanofiltration under different transmembrane pressures. *Journal of Environmental Sciences*, 25(2), 302–307.
- Zhang, Y., Dou, X.-M., Yang, M., He, H., Jing, C.-Y., & Wu, Z.-Y. (2010). Removal of arsenate from water by using an Fe-Ce oxide adsorbent: Effects of coexistent fluoride and phosphate. *Journal of Hazardous Materials*, 179(1–3), 208–214.
- Zhang, Y., Dou, X., Zhao, B., Yang, M., Takayama, T., & Kato, S. (2010). Removal of arsenic by a granular Fe-Ce oxide adsorbent: Fabrication conditions and performance. *Chemical Engineering Journal*, 162(1), 164–170.
- Zhang, G., He, Z., & Xu, W. (2012). A low-cost and high efficient zirconium-modified-Na-attapulgite adsorbent for fluoride removal from aqueous solutions. *Chemical Engineering Journal*, 183, 315–324.
- Zhang, F., Jin, Q., & Chan, S.-W. (2004). Ceria nanoparticles: Size, size distribution, and shape. *Journal of Applied Physics*, 95(8), 4319–4326.
- Zhang, G., Qu, J., Liu, H., Liu, R., & Wu, R. (2007). Preparation and evaluation of a novel Fe-Mn binary oxide adsorbent for effective arsenite removal. *Water Research*, 41(9), 1921–1928.
- Zhang, Y., Xu, Y., Zhang, S., Zhang, Y., & Xu, Z. (2012). Study on a novel composite membrane for treatment of sewage containing oil. *Desalination*, 299, 63–69.
- Zhang, Y., Yang, M., Dou, X.-M., He, H., & Wang, D.-S. (2005). Arsenate adsorption on an Fe-Ce bimetal oxide adsorbent: Role of surface properties. *Environmental Science & Technology*, 39(18), 7246–7253.
- Zhang, Y., Yang, M., & Huang, X. (2003). Arsenic(V) removal with a Ce(IV)-doped iron oxide adsorbent. *Chemosphere*, 51(9), 945–952.

- Zhang, X., Zhang, J., Wang, R., & Liu, Z. (2004). Cationic surfactant directed polyaniline/CNT nanocables: Synthesis, characterization, and enhanced electrical properties. *Carbon*, 42(8–9), 1455–1461.
- Zhang, J., Zhao, B., & Schreiner, B. (2016). *Separation hydrometallurgy of rare earth elements*. Switzerland: Springer.
- Zhang, L., Zhu, T., Liu, X., & Zhang, W. (2016). Simultaneous oxidation and adsorption of As(III) from water by cerium modified chitosan ultrafine nanobiosorbent. *Journal of Hazardous Materials*, 308, 1–10.
- Zheng, Y.-M., Yu, L., Wu, D., & Paul Chen, J. (2012). Removal of arsenite from aqueous solution by a zirconia nanoparticle. *Chemical Engineering Journal*, 188, 15–22.
- Zhong, L.-S., Hu, J.-S., Cao, A.-M., Liu, Q., Song, W.-G., & Wan, L.-J. (2007). 3D flower-like ceria micro/nanocomposite structure and its application for water treatment and CO removal. *Chemistry of Materials*, 19(7), 1648–1655.
- Zhou, Y., & Rahaman, M. (1993). Hydrothermal synthesis and sintering of ultrafine CeO₂ powders. *Journal of Materials Research*, 8(07), 1680–1686.
- Zhu, H.-Y., Jiang, R., Xiao, L., & Li, W. (2010). A novel magnetically separable γ -Fe₂O₃/crosslinked chitosan adsorbent: Preparation, characterization and adsorption application for removal of hazardous azo dye. *Journal of Hazardous Materials*, 179(1–3), 251–257.
- Zhu, Y., Murali, S., Cai, W., Li, X., Suk, J. W., Potts, J. R., & Ruoff, R. S. (2010). Graphene and graphene oxide: Synthesis, properties, and applications. *Advanced Materials*, 22(35), 3906–3924.